PICO

PROBE OF INFLATION
AND COSMIC ORIGINS

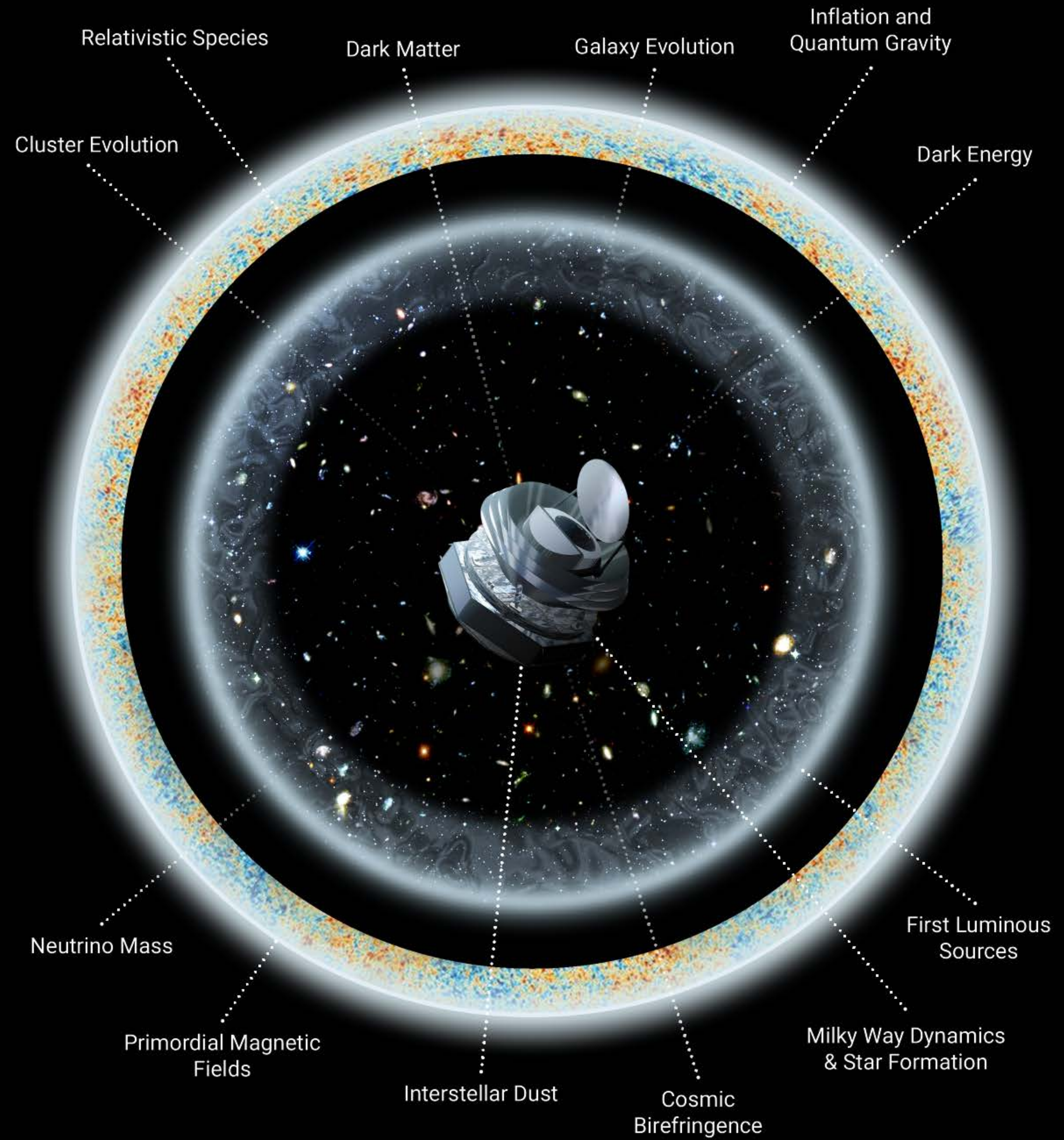

Shaul Hanany
University of Minnesota

https://z.umn.edu/picomission **http://z.umn.edu/picoendorse**

- Concept for Probe-Scale, next decade space mission
- Probe-scale: \$400M - \$1000M
- Concept development supported by NASA (05/2017 - 12/2018)
- Product: a report to the US Astro2020 decadal panel

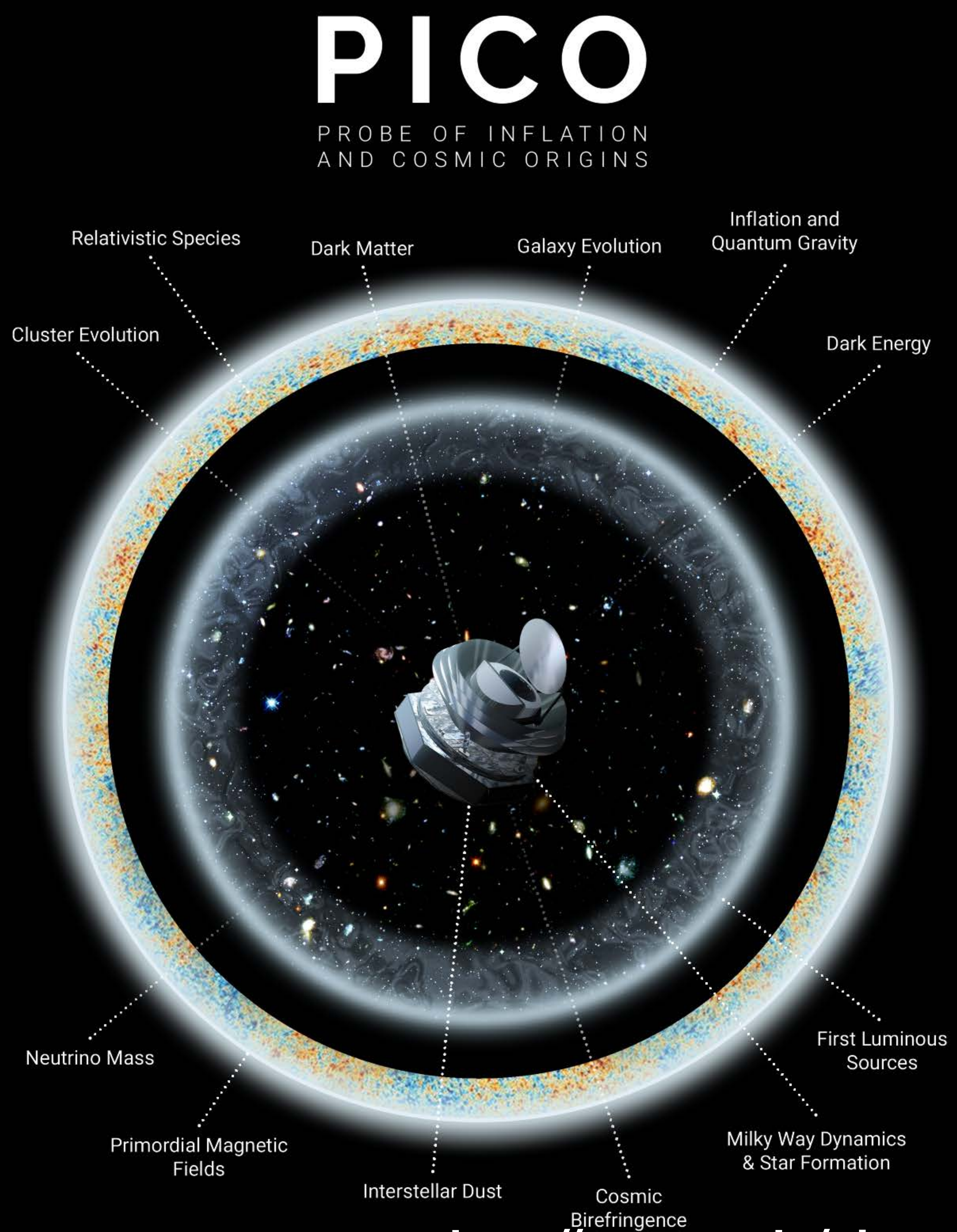

https://z.umn.edu/picomission

http://z.umn.edu/picoendorse

PICO

PROBE OF INFLATION

Report from a Probe-Scale Mission Study
January, 2019

Principal Investigator: Shaul Hanany [48]

Steering Committee: Charles Bennett [23], Scott Dodelson [5], Lyman Page [31]

Executive Committee: James Bartlett [1,22], Nick Battaglia [8], Jamie Bock [2,22], Julian Borrill [26,37], David Chuss [53], Brendan P. Crill [22], Jacques Delabrouille [1,20], Mark Devlin [50], Laura Fissel [29], Raphael Flauger [43], Dan Green [41], J. Colin Hill [6,17], Johannes Hubmayr [28], William Jones [31], Lloyd Knox [42], Al Kogut [27], Charles Lawrence [22], Jeff McMahon [47], Tim Pearson [2], Clem Pryke [48], Marcel Schmittfull [17], Amy Trangsrud [22], Alexander van Engelen [3]

Authors

Marcelo Alvarez [26,41]
Emmanuel Artis [20]
Peter Ashton [25,26,41]
Jonathan Aumont [19]
Ranajoy Banerji [49]
R. Belen Barreiro [18]
James G. Bartlett [1,22]
Soumen Basak [34]
Nick Battaglia [8]
Jamie Bock [2,22]
Kimberly K. Boddy [23]
Matteo Bonato [13]
Julian Borrill [26,37]
François Bouchet [15]
François Boulanger [10]
Blakesley Burkhart [32]
Jens Chluba [21]
David Chuss [53]
Susan E. Clark [17]
Joelle Cooperrider [22]
Brendan P. Crill [22]
Gianfranco De Zotti [14]
Jacques Delabrouille [1,20]
Eleonora Di Valentino [46]
Joy Didier [51]
Olivier Doré [22,2]
Josquin Errard [1]
Tom Essinger-Hileman [27]
Stephen Feeney [6]
Jeffrey Filippini [45]
Laura Fissel [29]
Raphael Flauger [43]
Vera Gluscevic [44]
Kris Gorski [22]
Dan Green [41]
Shaul Hanany [48]
Brandon Hensley [31]
Diego Herranz [18]
J. Colin Hill [6,17]
Eric Hivon [15]
Renée Hložek [9]
Johannes Hubmayr [28]
Bradley R. Johnson [7]
William Jones [31]
Terry Jones [48]
Lloyd Knox [42]
Al Kogut [27]
Marcos López-Caniego [11]
Charles Lawrence [22]
Alex Lazarian [52]
Zack Li [31]
Mathew Madhavacheril [31]
Jean-Baptiste Melin [20]
Joel Meyers [36]
Calum Murray [1]
Mattia Negrello [4]
Giles Novak [30]
Roger O'Brient [22,2]
Christopher Paine [22]
Tim Pearson [2]
Levon Pogosian [35]
Clem Pryke [48]
Giuseppe Puglisi [24,38]
Mathieu Remazeilles [21]
Graca Rocha [22]
Marcel Schmittfull [17]
Douglas Scott [40]
Ian Stephens [12]
Brian Sutin [22]
Maurizio Tomasi [39]
Amy Trangsrud [22]
Alexander van Engelen [3]
Flavien Vansyngel [16]
Qi Wen [48]
Siyao Xu [52]
Karl Young [48]
Andrea Zonca [33]

Endorsers

Maximilian Abitbol
Zeeshan Ahmed
David Alonso
Jason Austermann
Darcy Barron
Daniel Baumann
Karim Benabed
Bradford Benson
Paolo de Bernardis
Marco Bersanelli
Federico Bianchini
Colin Bischoff
J. Richard Bond
Sean Bryan
Carlo Burigana
Robert Caldwell
Xingang Chen
Francis-Yan Cyr-Racine
Tijmen de Haan
Cora Dvorkin
Ivan Soares Ferreira
Aurelien Fraisse
Vincent Vennin
Licia Verde
Patricio Vielva
Andrei V. Frolov
Ken Ganga
Silvia Galli
Ken Ganga
Tuhin Ghosh
Sunil Golwala
Riccardo Gualtieri
Jon E. Gudmundsson
Nikhel Gupta
Sophie Henrot-Versillé
Thiem Hoang
Kevin M. Huffenberger
Marc Kamionkowski
Reijo Keskitalo
Rishi Khatri
Theodore Kisner
Arthur Kosowsky
Ely Kovetz
Kerstin Kunze
Guilaine Lagache
Daniel Lenz
François Levrier
Benjamin Wallisch
Benjamin Wandelt
Scott Watson
Marilena Loverde
Philip Lubin
Juan Macias-Perez
Nazzareno Mandolesi
Carlos Martins
Silvia Masi
P. Daniel Meerburg
Amber Miller
Lorenzo Moncelsi
Pavel Motloch
Tony Mroczkowski
Suvodip Mukherjee
Johanna Nagy
Pavel Naselsky
Federico Nati
Paolo Natoli
Michael Niemack
Elena Orlando
Francesco Piacentini
Nicolas Ponthieu
Giuseppe Puglisi
Benjamin Racine
Rien van de Weygaert
Edward J. Wollack
Siavash Yasini
Christian Reichardt
Christophe Ringeval
Karwan Rostem
Anirban Roy
Jose-Alberto Rubino-Martin
Maria Salatino
Benjamin Saliwanchik
Neelima Sehgal
Sarah Shandera
Erik Shirokoff
Anže Slosar
Tarun Souradeep
Suzanne Staggs
George Stein
Aritoki Suzuki
Eric Switzer
Andrea Tartari
Grant Teply
Peter Timbie
Matthieu Tristram
Caterina Umiltà

Primordial Magnetic Fields

Interstellar Dust

- **Open community effort**
- **Contributions/endorsements still accepted**

https://z.umn.edu/picomission

http://z.umn.edu/picoendorse

PICO in Brief

- Millimeter/submillimeter-wave, polarimetric survey of the entire sky
- 21 bands between 20 GHz and 800 GHz
- 1.4 m aperture telescope
- Diffraction limited resolution: 38’ to 1’
- 13,000 transition edge sensor bolometers + multiplexed readouts
- 5 year survey from L2
- Requirement: 0.87 uK*arcmin, 3300 *Planck* misions
- Current estimate: 0.61 uK*arcmin, 6700 *Planck* misions

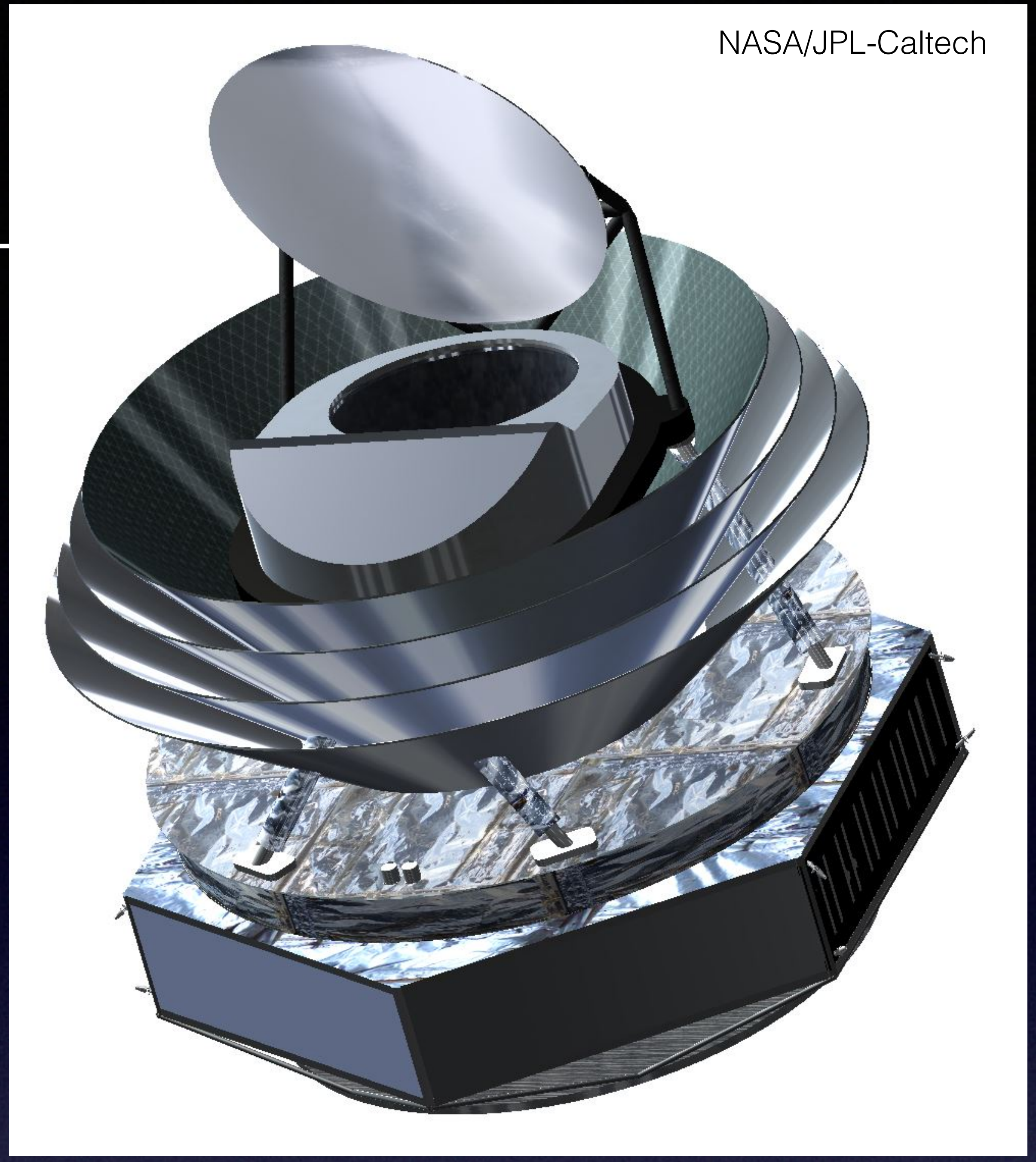

Sutin et al. SPIE Vol.10698; 1808.01368

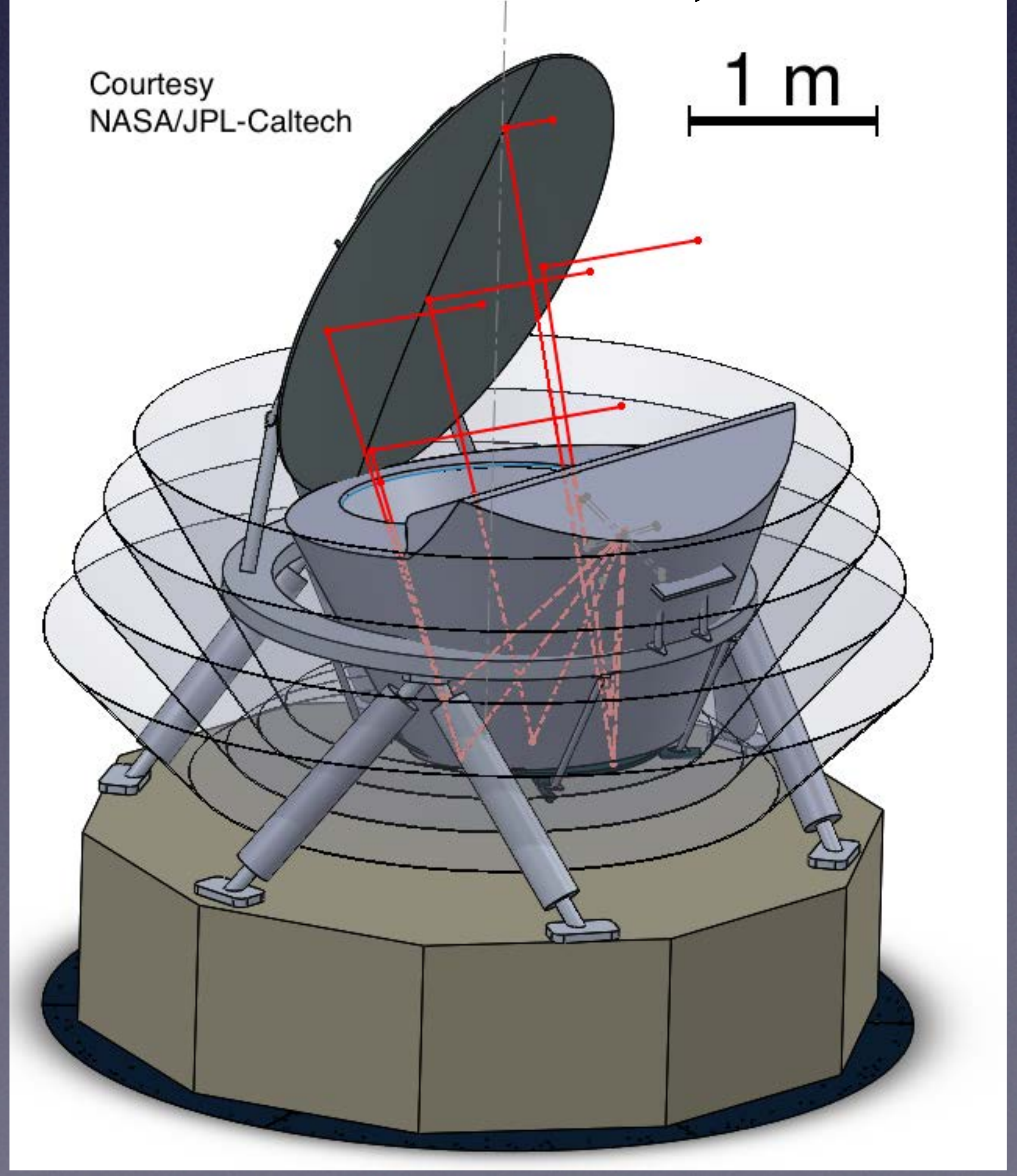

PICO Science Objective - 1: Inflation r

- The classes of models that naturally explain n_s, and have a scale of M_p or larger in the potential have $r \gtrsim 5 \times 10^{-4}$
- Goal: detect $r = 5 \times 10^{-4}\,(5\sigma)$

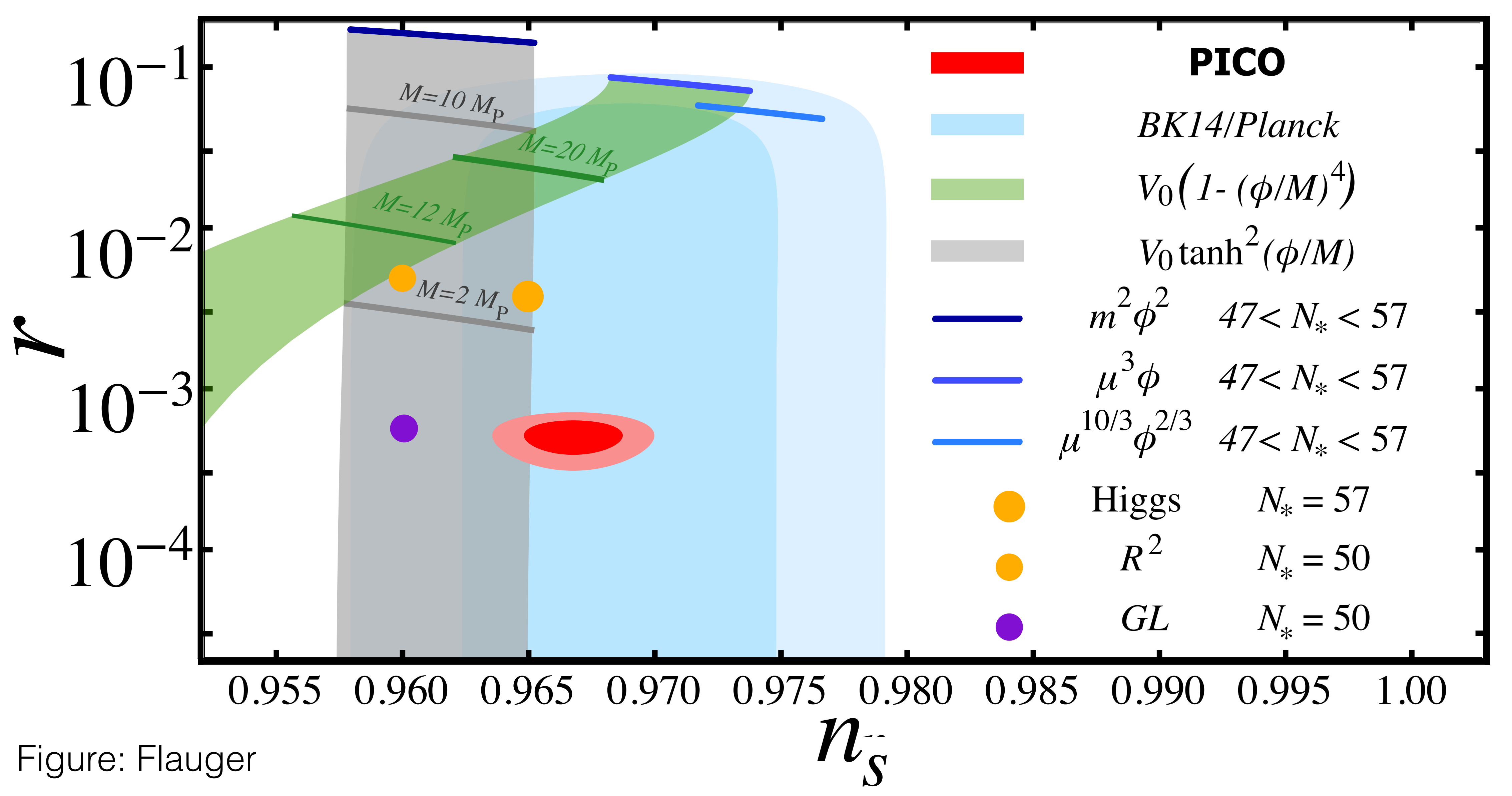

Figure: Flauger

PICO Science Objective - 1: Inflation-r

- The classes of models that naturally explain n_s, and have a scale of M_p or larger in the potential have $r \gtrsim 5 \times 10^{-4}$
- Goal: detect $r = 5 \times 10^{-4} \, (5\sigma)$

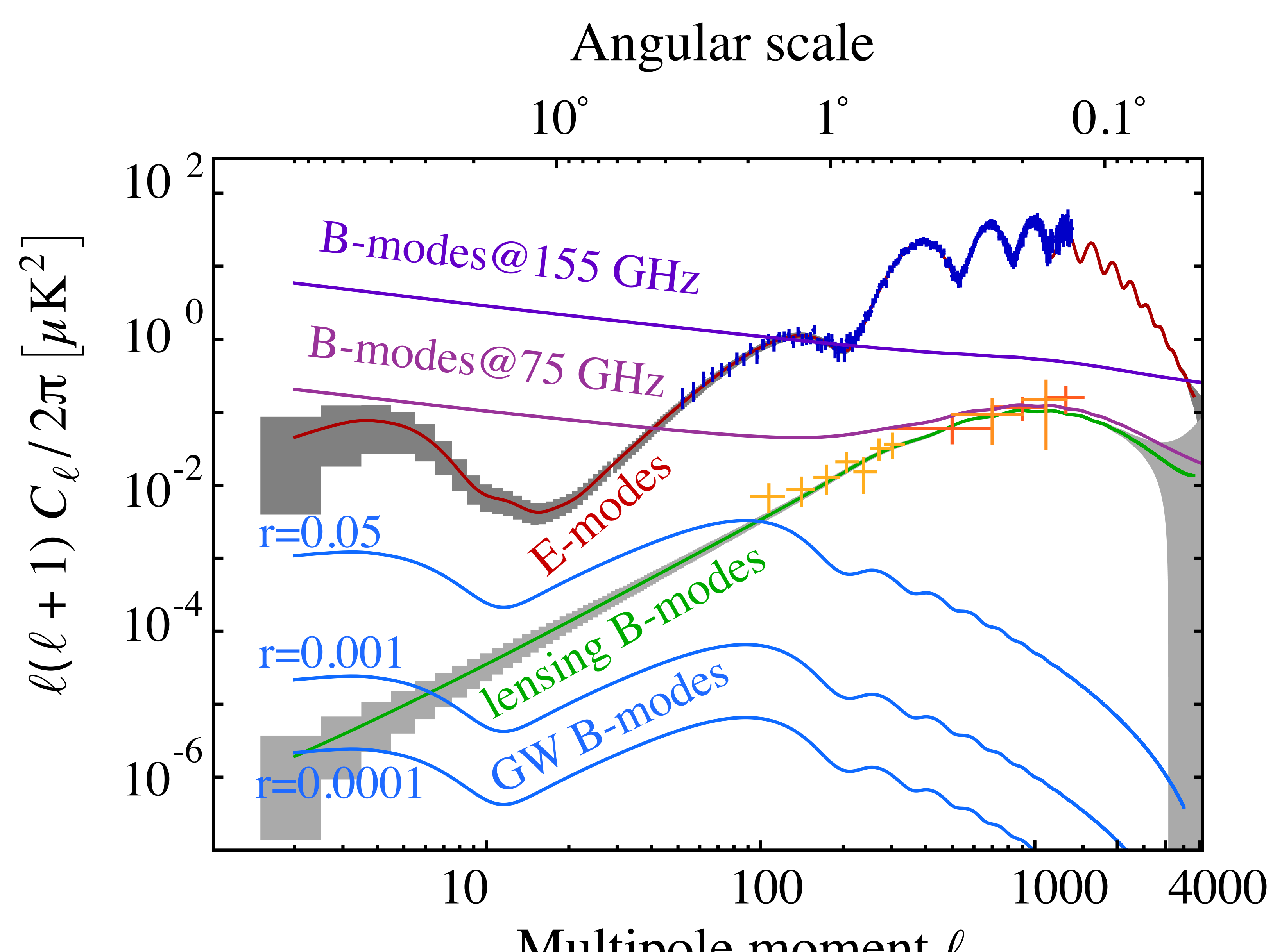

Figure: R. Flauger

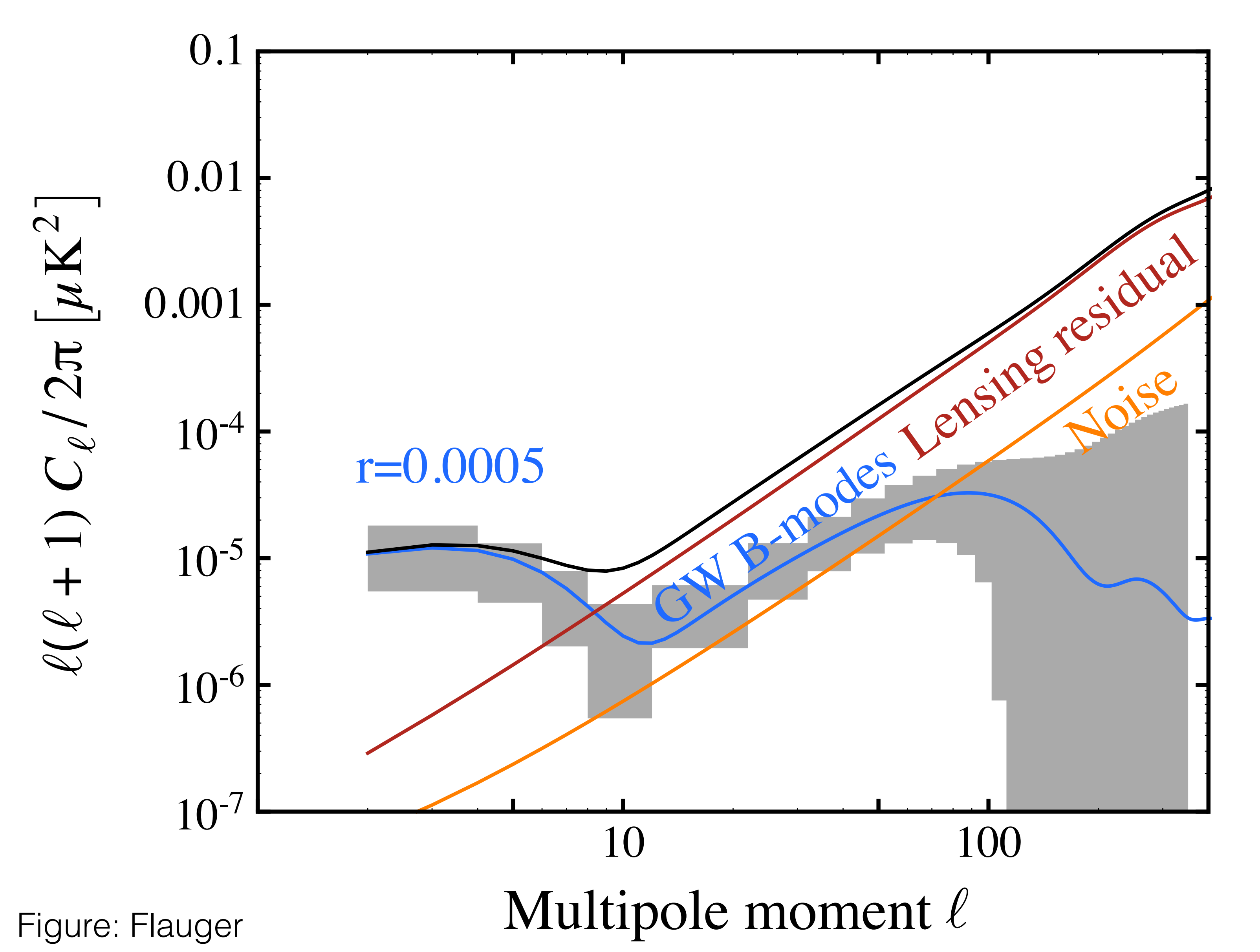

Figure: Flauger

PICO Science Objective - 1: Can the Foregrounds be Handled

- Fisher forecast that includes correlated foregrounds, foreground separation, 40% sky, and delensing gives $\sigma(r) = 2 \times 10^{-5}$

- Map based simulation (PySM model), r=0, 50% of sky, 15% lensing, PICO noise, GNILC foreground removal with 21 bands

- Lowest \ell has x2 bias relative to lensing, x10 lower than $r = 5 \times 10^{-4}$

- For \ell=100, residual is x4 lower

- More models, smaller sky patches, other techniques are all in progress

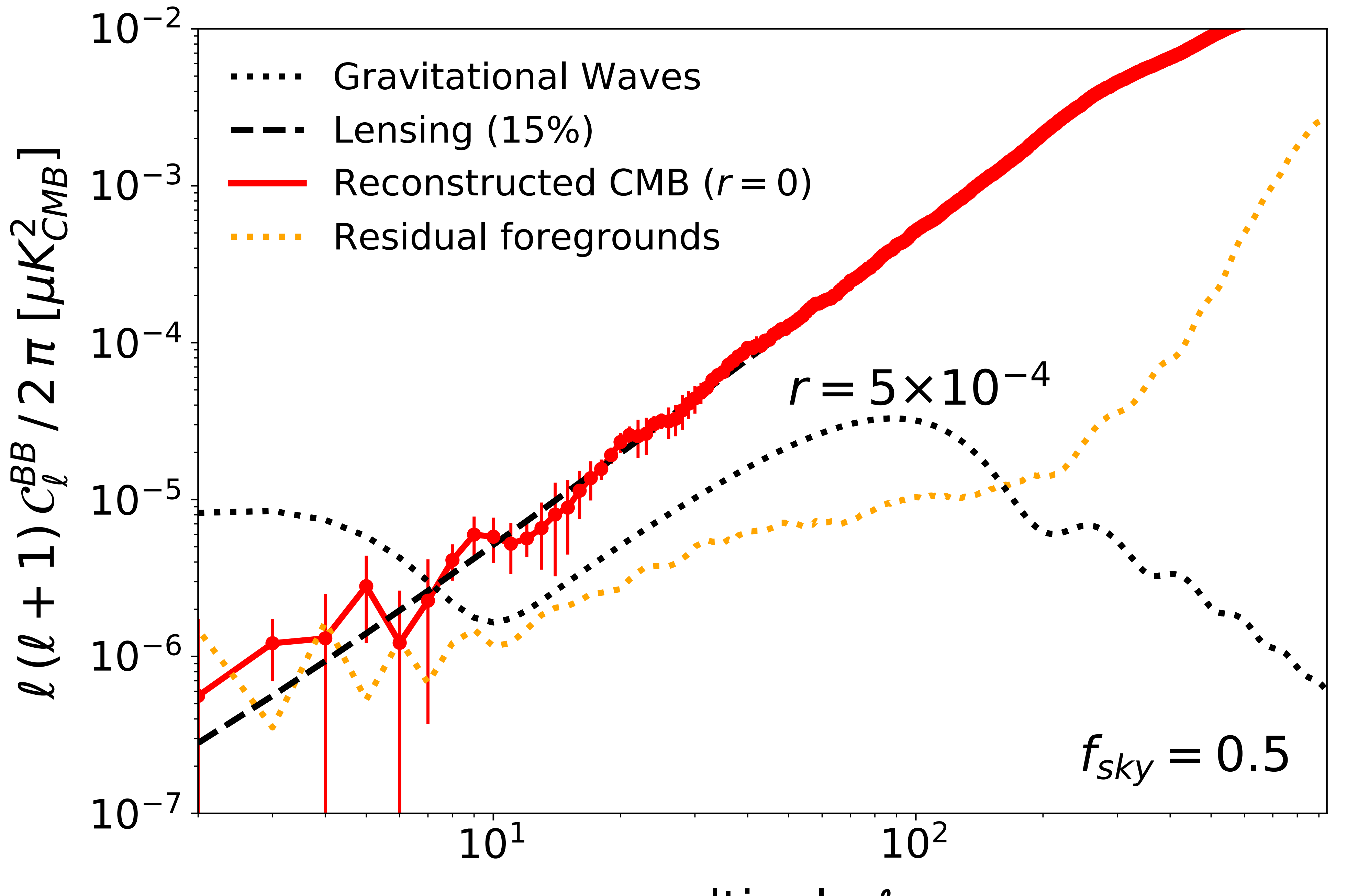

Figure: Remazeilles

PICO Science Objective - 2: Inflation-Models

- No detection: rule out all models with scale M_p or larger at high significance
- Model of inflation differ in their reheating scenarios
- Measure n_s and n_{run} with

$$\sigma(n_s) = 0.0015 \quad \sigma(n_{run}) = 0.002$$

- Give 3σ discrimination between models that have different reheating scenarios

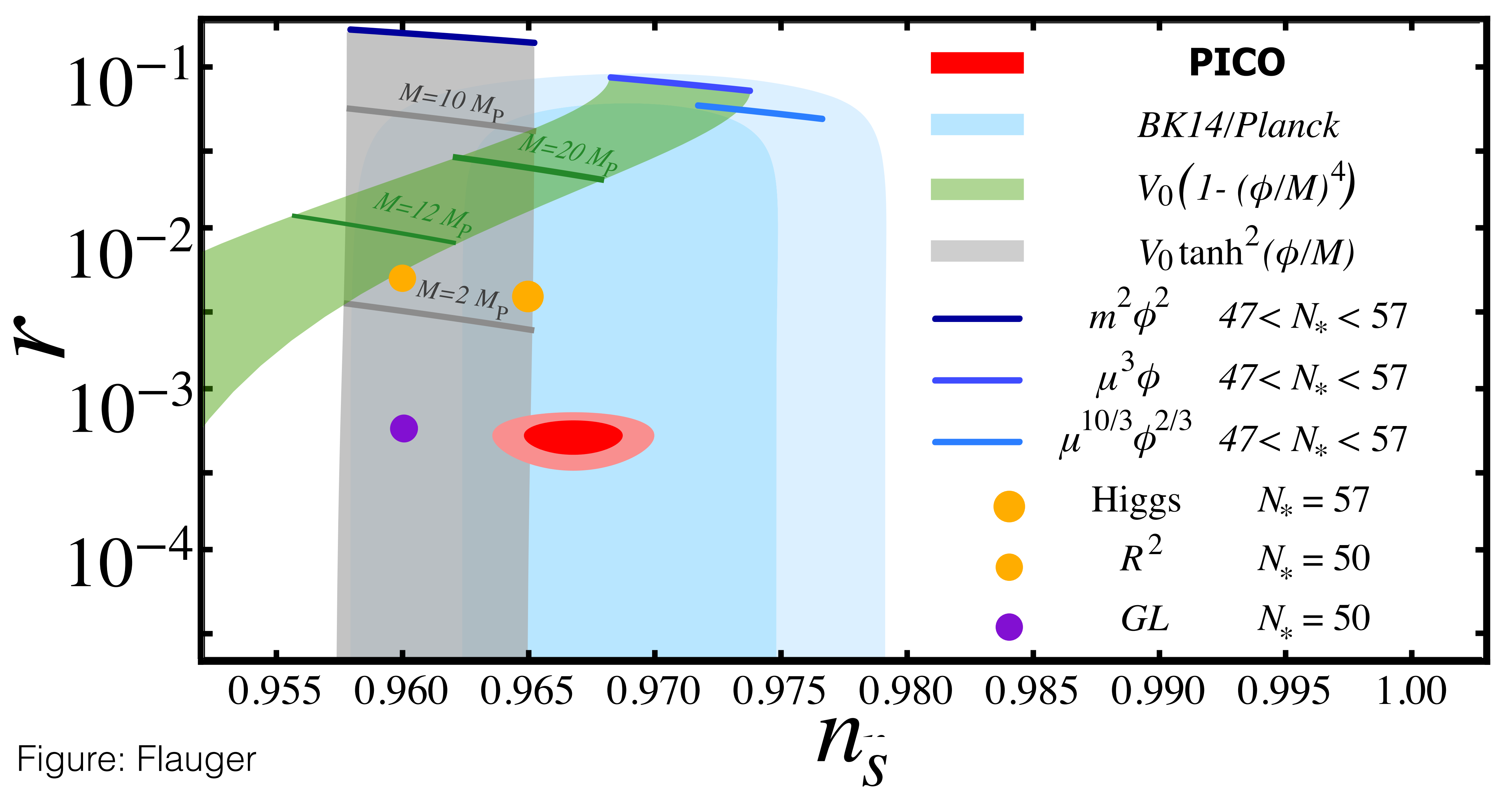

Figure: Flauger

PICO Science Objective - Inflation - non-Gaussianity

- Single-field models have nearly Gaussian fluctuations, $f_{\rm NL}^{\rm local} < 1$
- Detection of $f_{\rm NL}^{\rm local} > 1$ evidence for multi-field inflation
- Planck: $f_{\rm NL}^{\rm local} = 0.8 \pm 5$
- PICO ϕ + LSST galaxies: $f_{\rm NL}^{\rm local} = 1\,(2\sigma)$
  - LSST: i<27, L_{min}>4
- PICO ϕ + LSST galaxies: $f_{\rm NL}^{\rm local} = 2\,(3\sigma)$
  - LSST: i<25.3, L_{min}>8

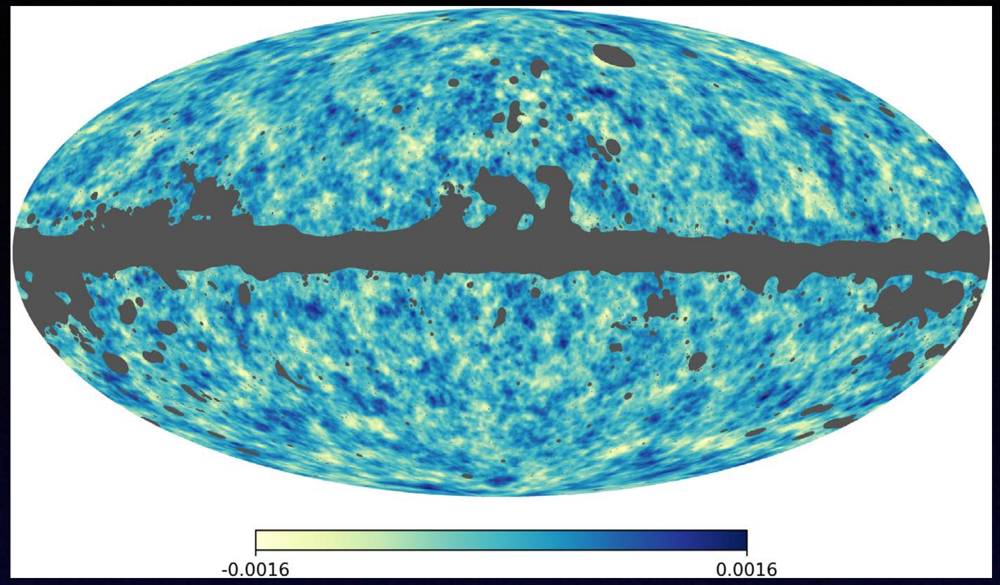

PICO Lensing

x


LSST Galaxies

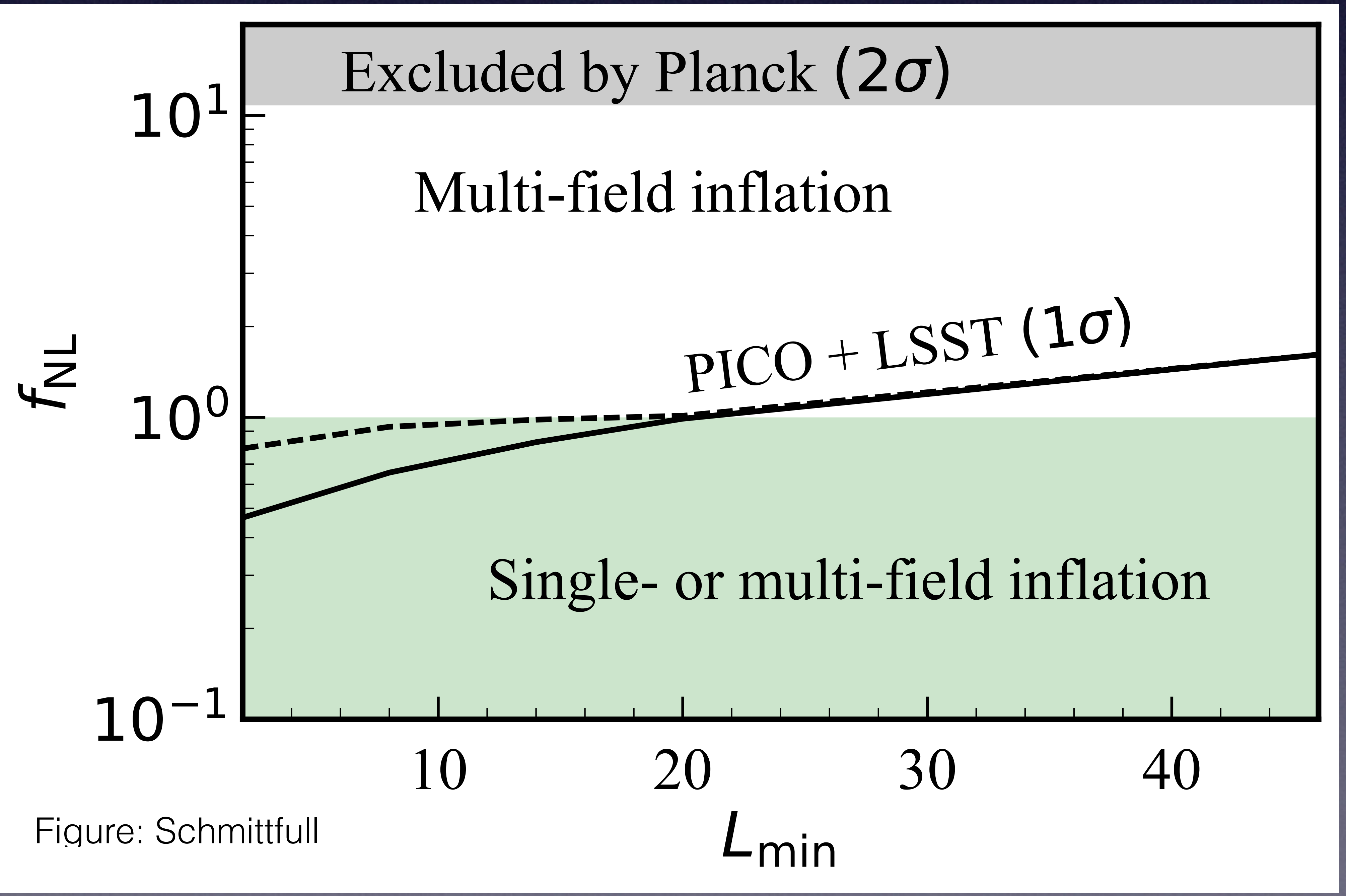

Figure: Schmittfull

PICO Science Objective - 3: Neutrino Mass

- Growth of structures is affected by sum of neutrino mass
- The map of projected gravitational potential is a sensitive probe of the growth of structures
- The lensing amplitude is proportional to
  - neutrino mass
  - matter density (BAO)
  - primordial perturbations power spectrum (degenerate with τ)
- PICO lensing map: SNR = 560 (planck SNR = 40)

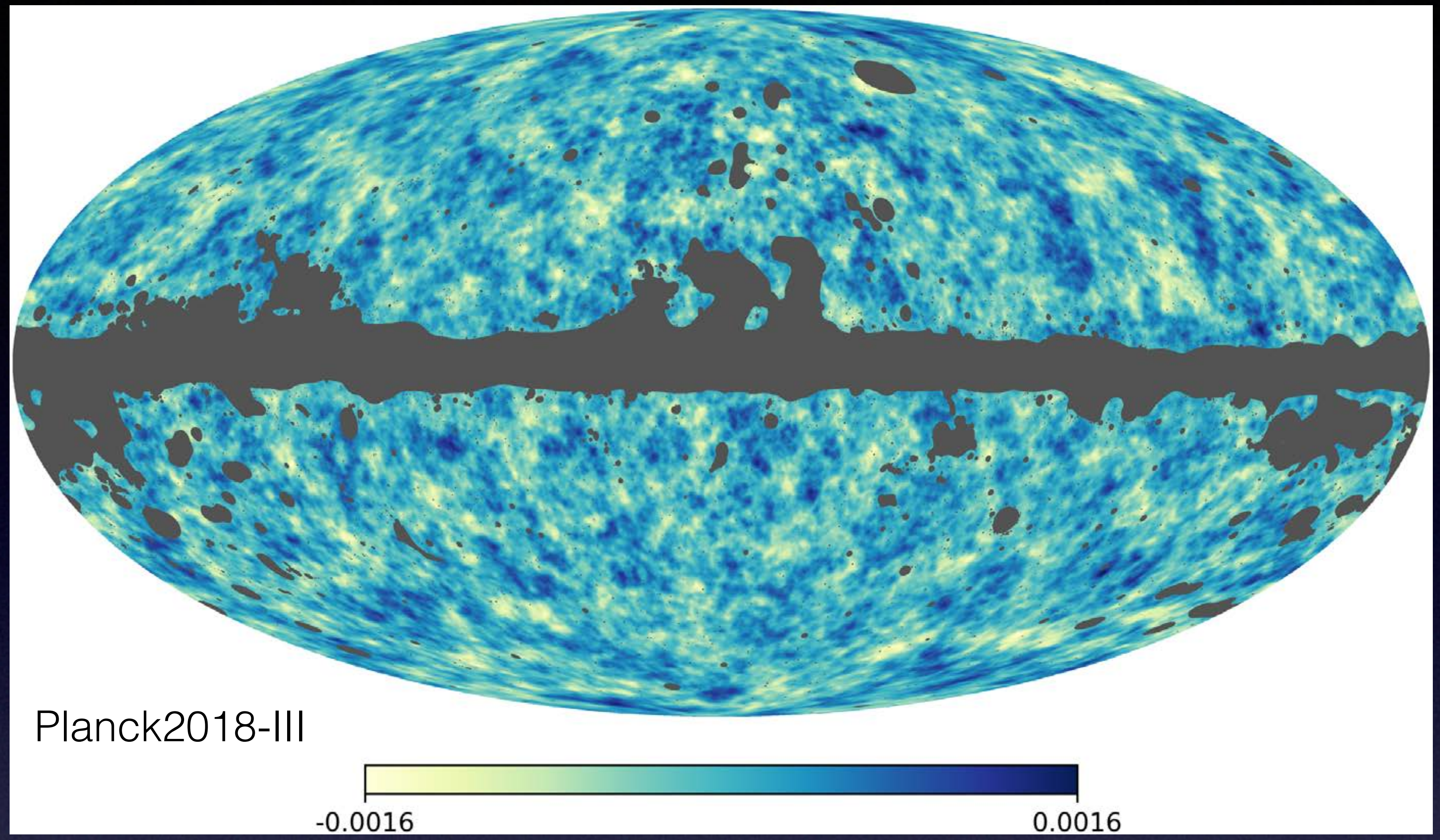

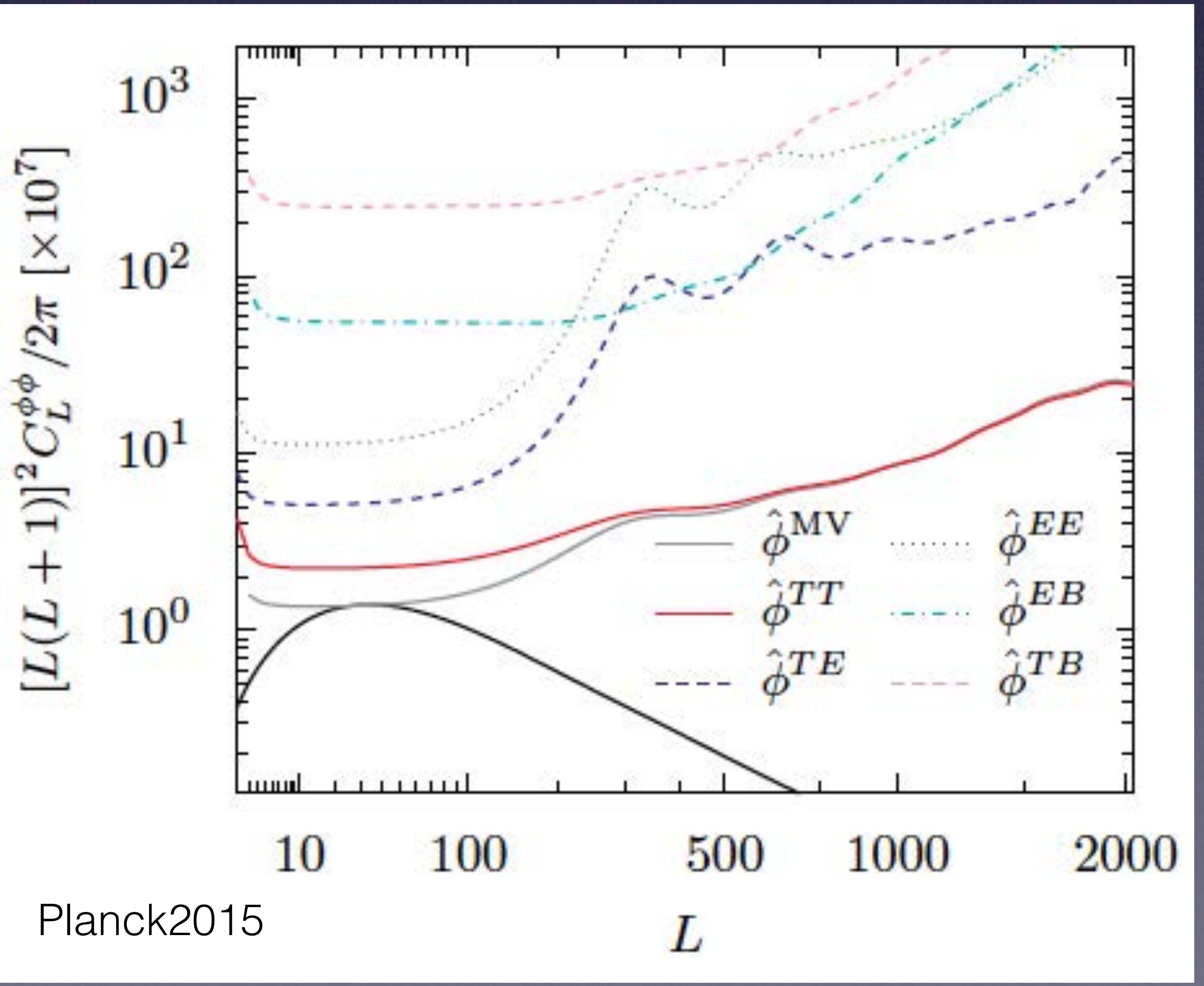

PICO Science Objective - 3: Neutrino Mass

- Growth of structures is affected by sum of neutrino mass
- The map of projected gravitational potential is a sensitive probe of the growth of structures
- The lensing amplitude is proportional to
  - neutrino mass
  - matter density (BAO)
  - primordial perturbations power spectrum (degenerate with τ)
- PICO lensing map: SNR = 560 (planck SNR = 40)

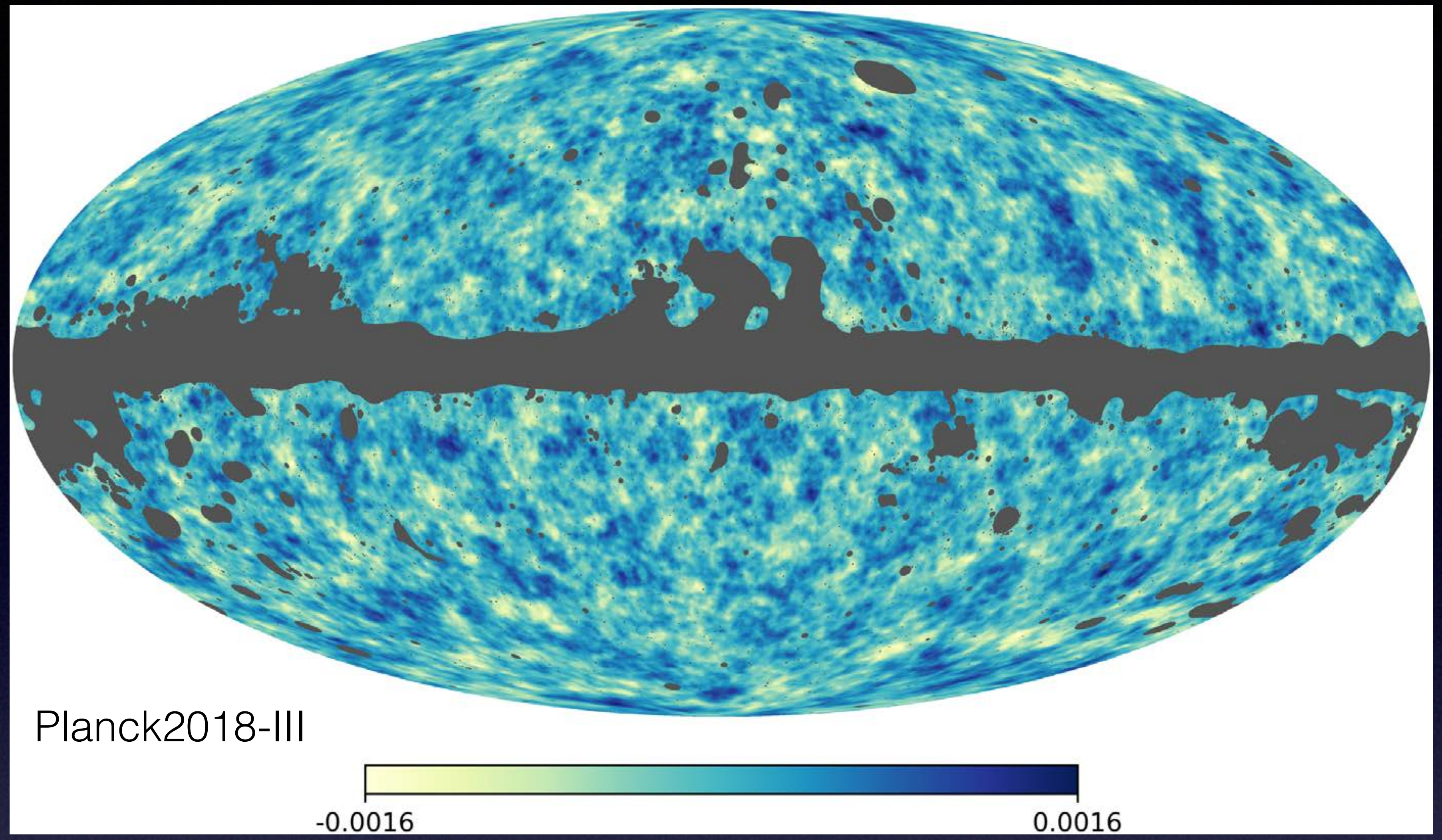

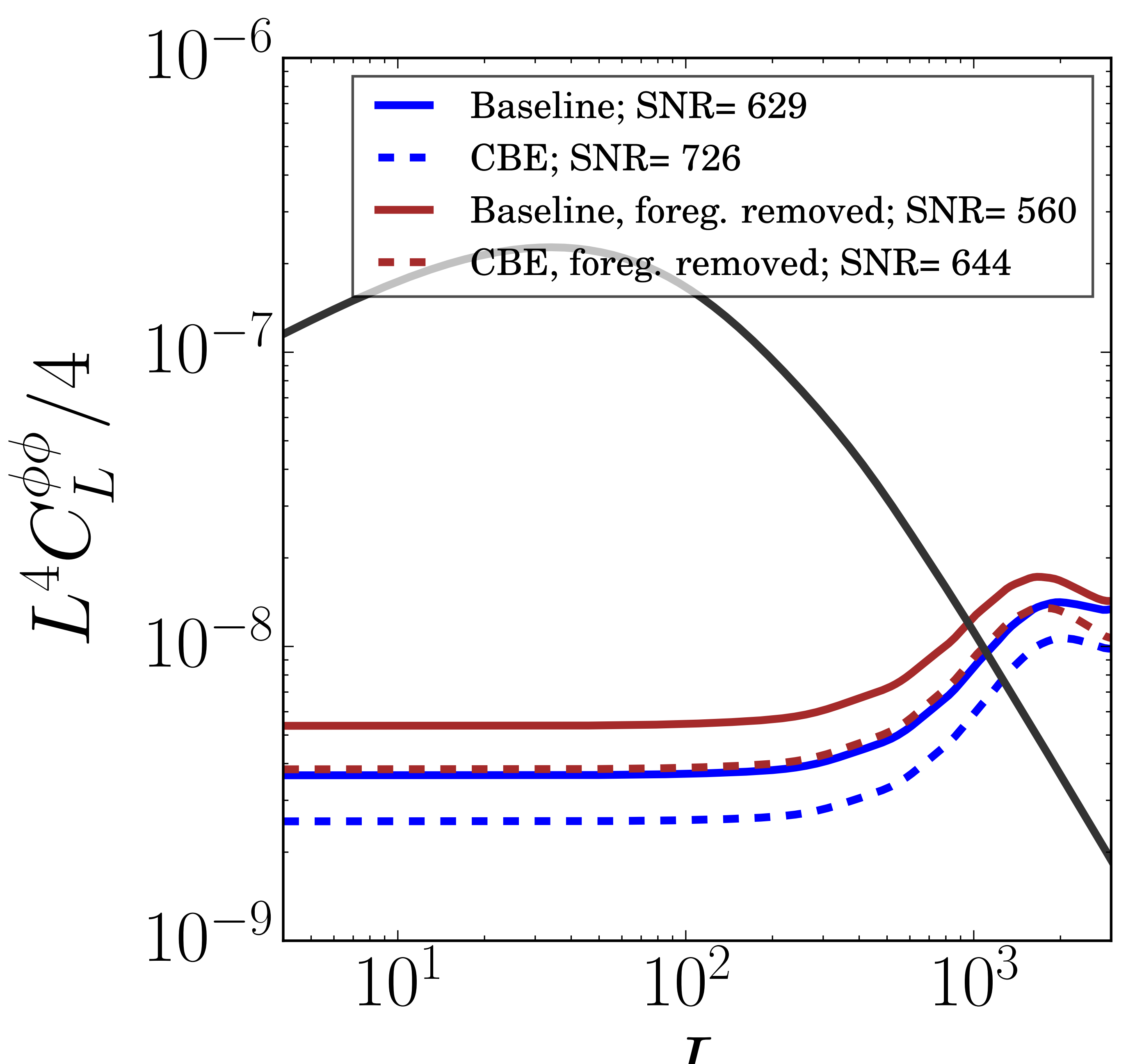

Figure: van Engelen

PICO Science Objective - 3: Neutrino Mass

- Growth of structures is affected by sum of neutrino mass
- The map of projected gravitational potential is a sensitive probe of the growth of structures
- The lensing amplitude is proportional to
  - neutrino mass
  - matter density (BAO)
  - primordial perturbations power spectrum (degenerate with τ)
- PICO lensing map: SNR = 560 (planck SNR = 40)
- PICO $\sigma(\tau) = 0.002$ CVL
- $\sigma\left(\Sigma m_{\nu}\right) = 14$ meV (one of three constraints)

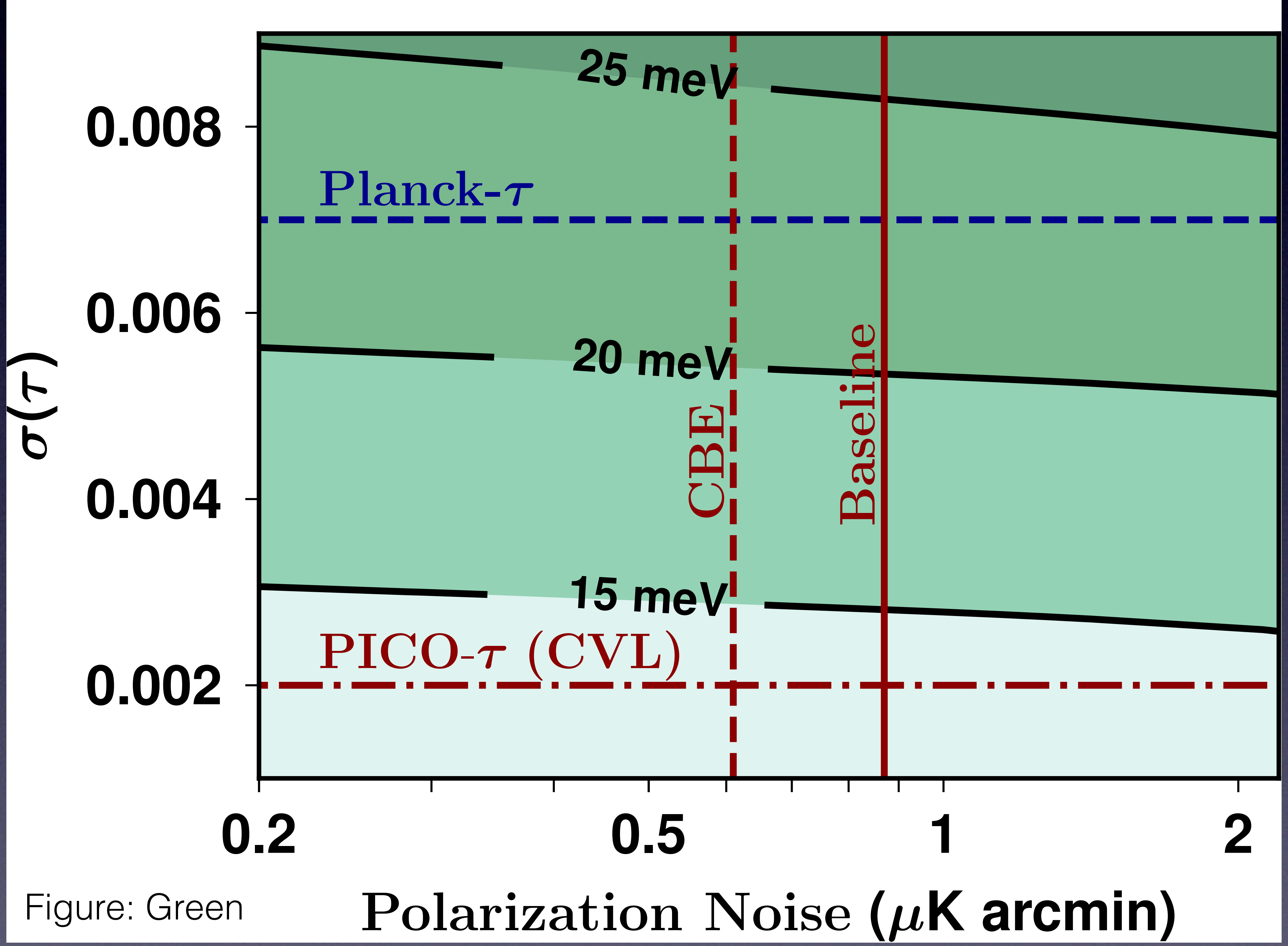

Figure: Green

PICO Science Objective - 4: New Particles

- Light species, beyond 3 neutrinos, could have existed in the early universe and fallen out of thermal equilibrium at high temperatures.
- CMB spectra are sensitive to the number of light species N_{eff}
- Only 3 neutrinos gives: Neff = 3.046
- Planck + BAO : 2.92 ± 0.36 (95%)
- PICO: $\Delta(N_{\text{eff}}) = 0.06\ (95\%)$

Change to nominal Neff with additional light species

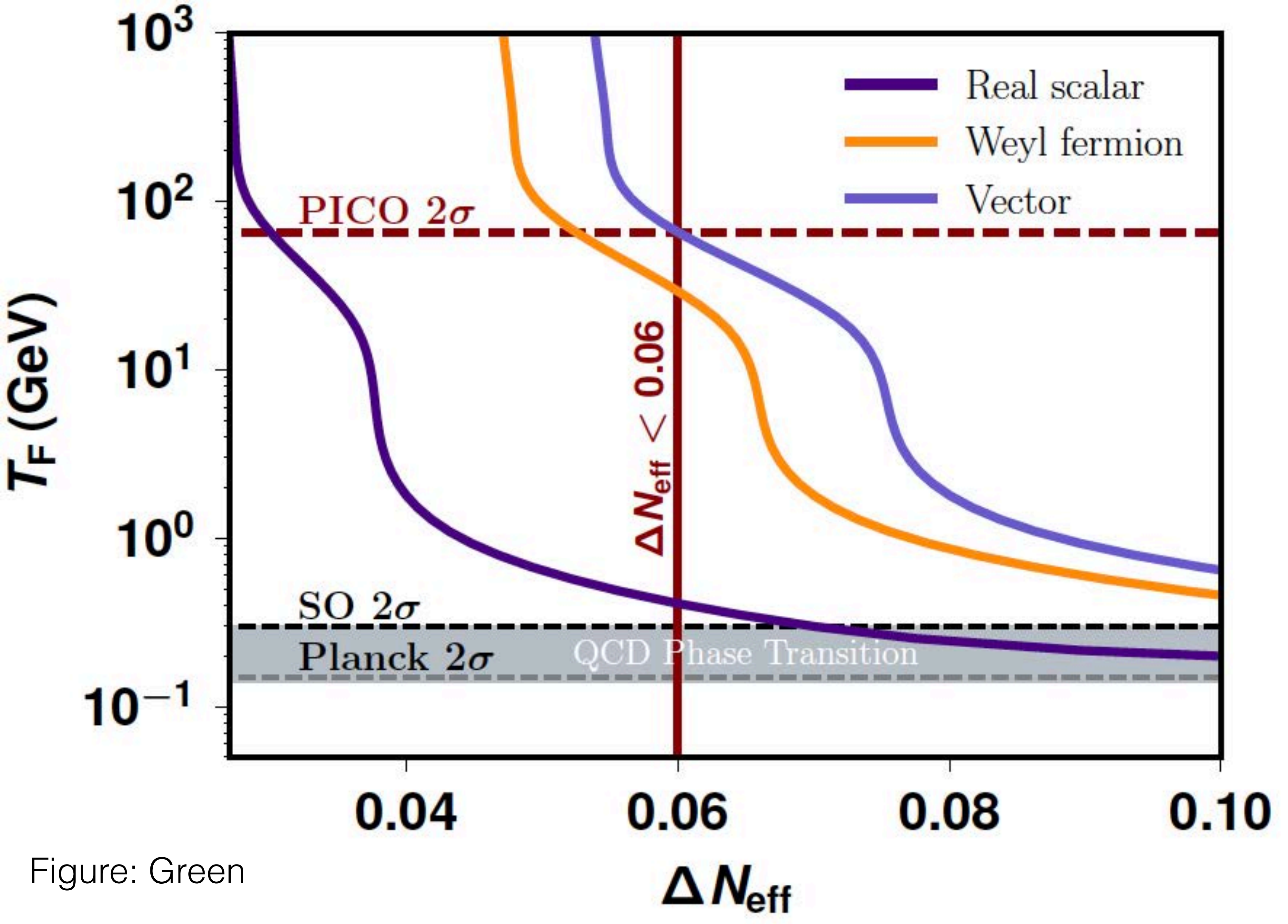

Figure: Green

PICO Science Objective - 5: First Luminous Sources

- Low ℓ EE -> probe of the optical depth to reionization
- PICO $\sigma(\tau) = 0.002$ CVL => determine z_{re}
- With kSZ (Δz_{re}) constrain models of reionization (kSZ from S3)

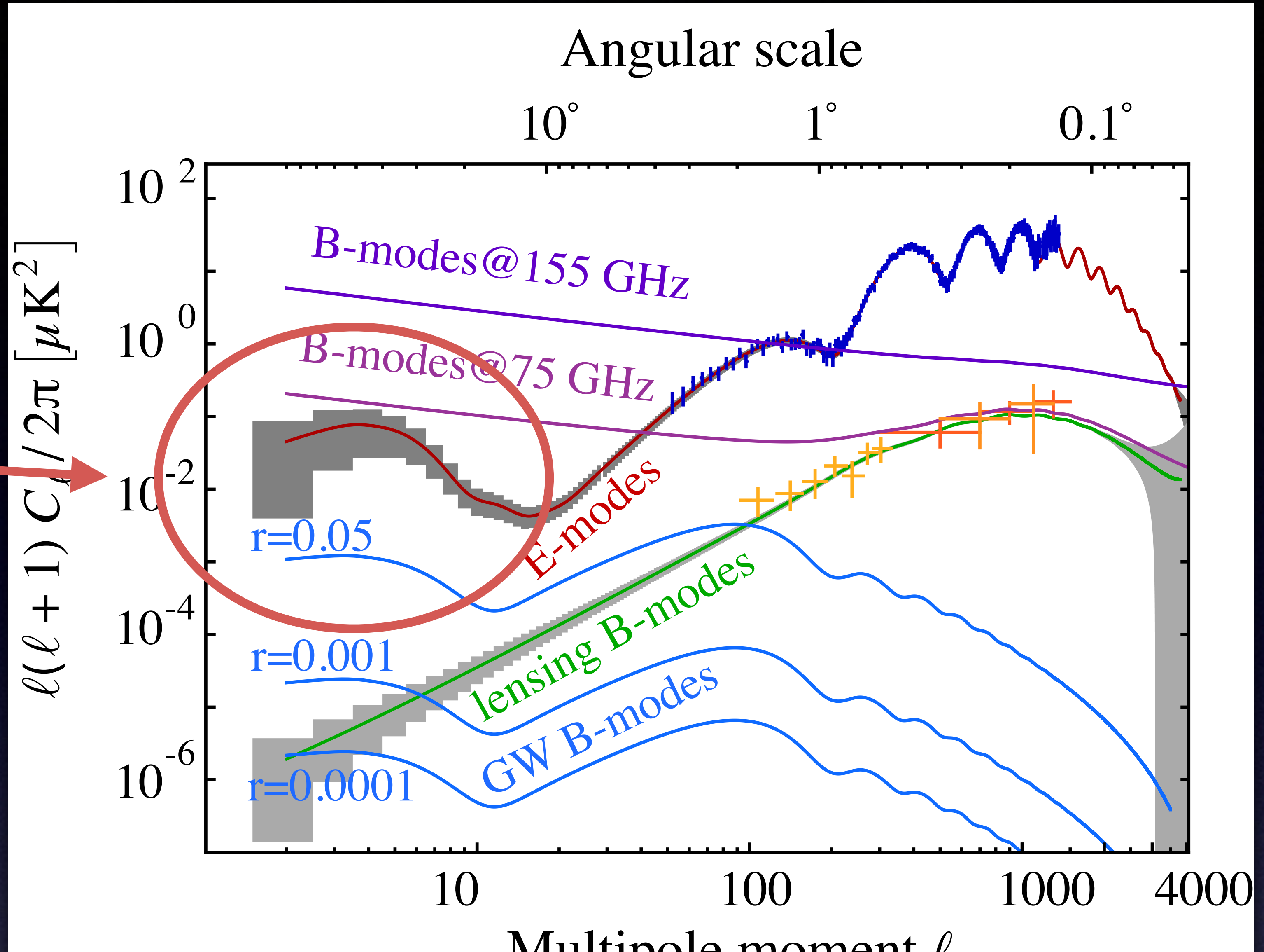

Figure: Flauger

Planck + S3

PICO + S3

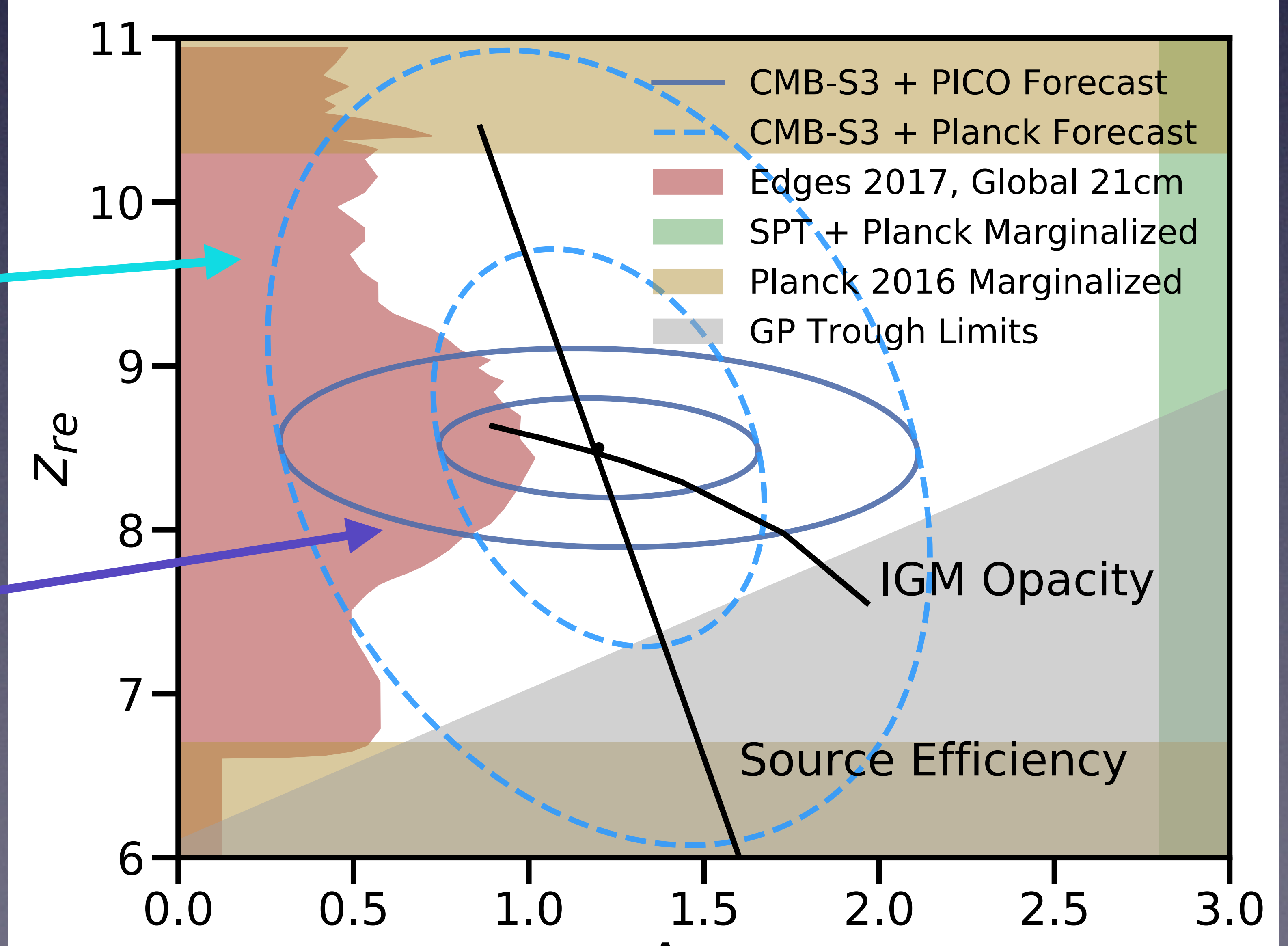

Figure: Battaglia + Alvarez

PICO Science Objective - 6: Composition of Interstellar Dust

- Carbons and silicates are major components
- Are there distinct populations, with distinct growth paths, or are the components completely mixed on the grains?
- PICO: 3% per component per frequency band
  - Support or rule out the distinct two component model
- Better characterization will lead to better separation of dust from B-mode science

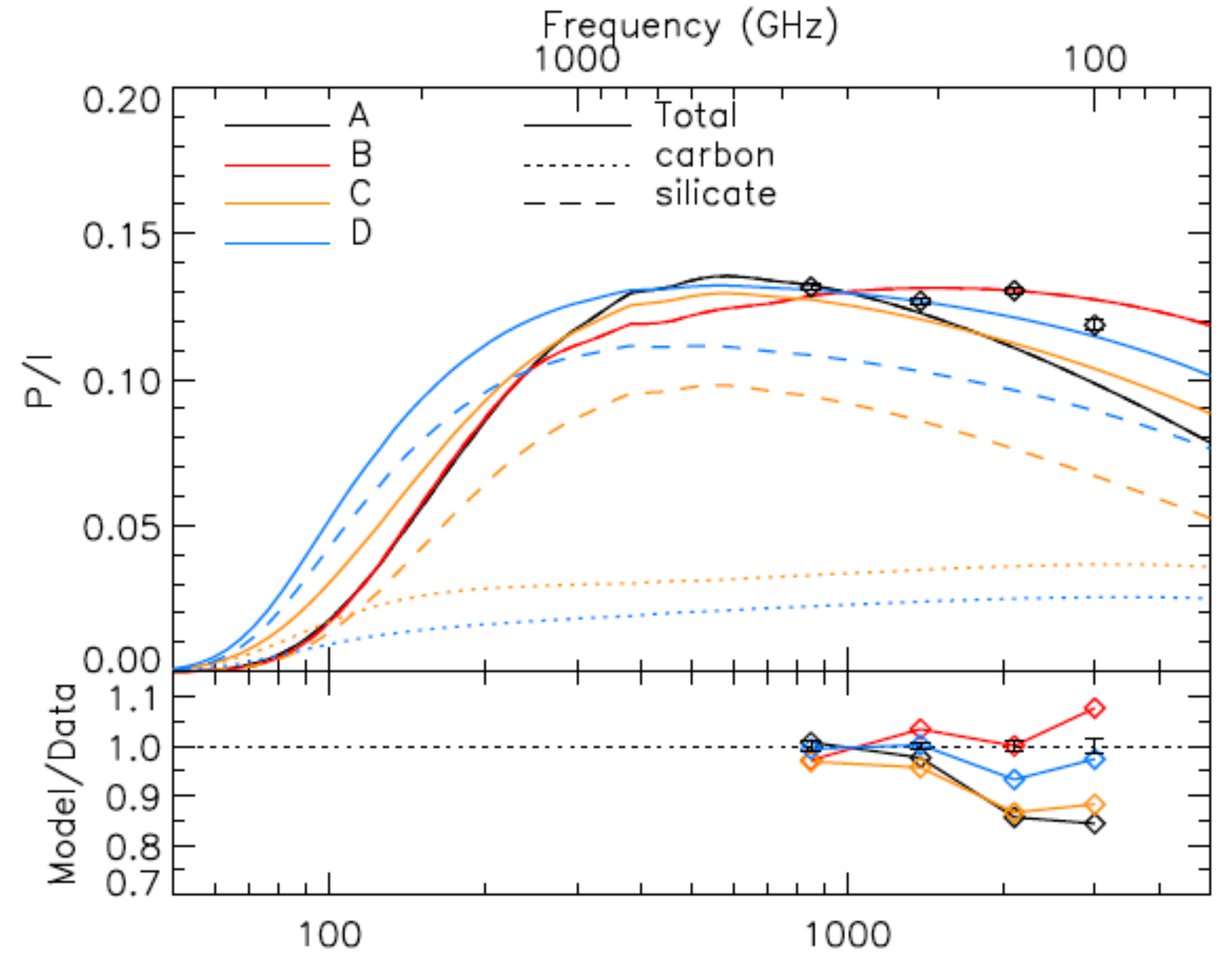

Guillet et al. 2018

PICO Science Objective - 6: Composition of Interstellar Dust

- Carbons and silicates are major components
- Are there distinct populations, with distinct growth paths, or are the components completely mixed on the grains?
- PICO: 3% per component per frequency band
  - Support or rule out the distinct two component model
- Better characterization will lead to better separation of dust from B-mode science

+6 lower frequency bands

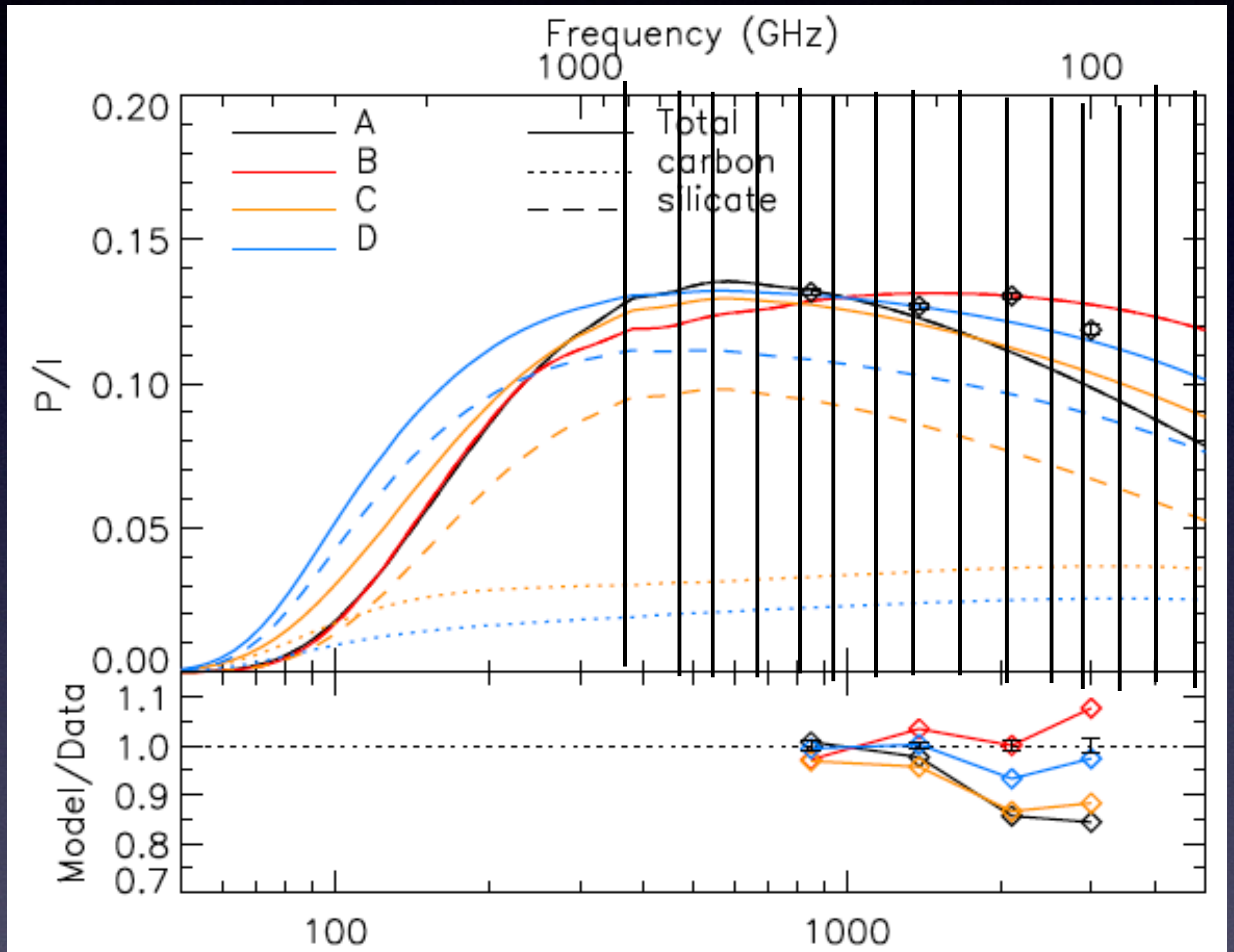

Guillet et al. 2018

PICO Science Objective - 7: Low Galactic Star Formation Efficiency

- Stars form at much lower rate than would be expected from gravitational collapse
- Turbulence, magnetic fields slow collapse from the diffuse ISM to molecular clouds, to star forming regions
- What is the ratio of energy stored in the magnetic field to that stored in turbulent motion over spatial scales from the diffuse ISM to dense cores?
- Need measurements of magnetic fields over scales of galaxy down to dense cores

PICO Science Objective - 7: Low Galactic Star Formation Efficiency

86,000,000 independent B field measurements
x1000 more than Planck

Figure: Chuss + Fissel

PICO Science : Galactic Magnetic fields

- Map magnetic fields in 70 external galaxies, with 100 measurements per galaxy (currently 2 are mapped)
- Map 10 nearby clouds with 0.1 pc resolution => scale of cloud cores (currently no data are available to connect magnetic fields in the diffuse ISM to that in cloud cores)

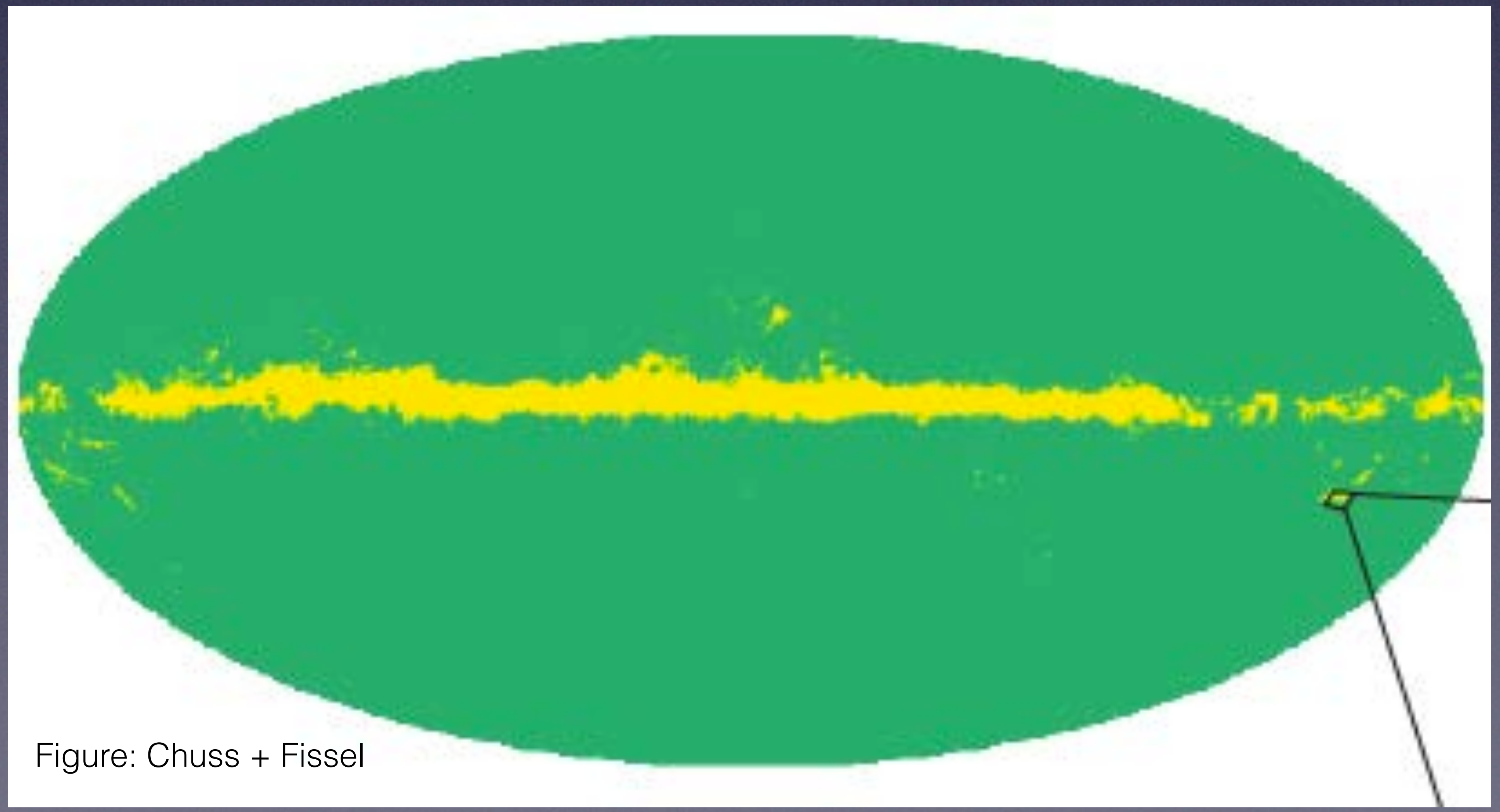

Figure: Chuss + Fissel

Factor of 10^4 in spatial scale

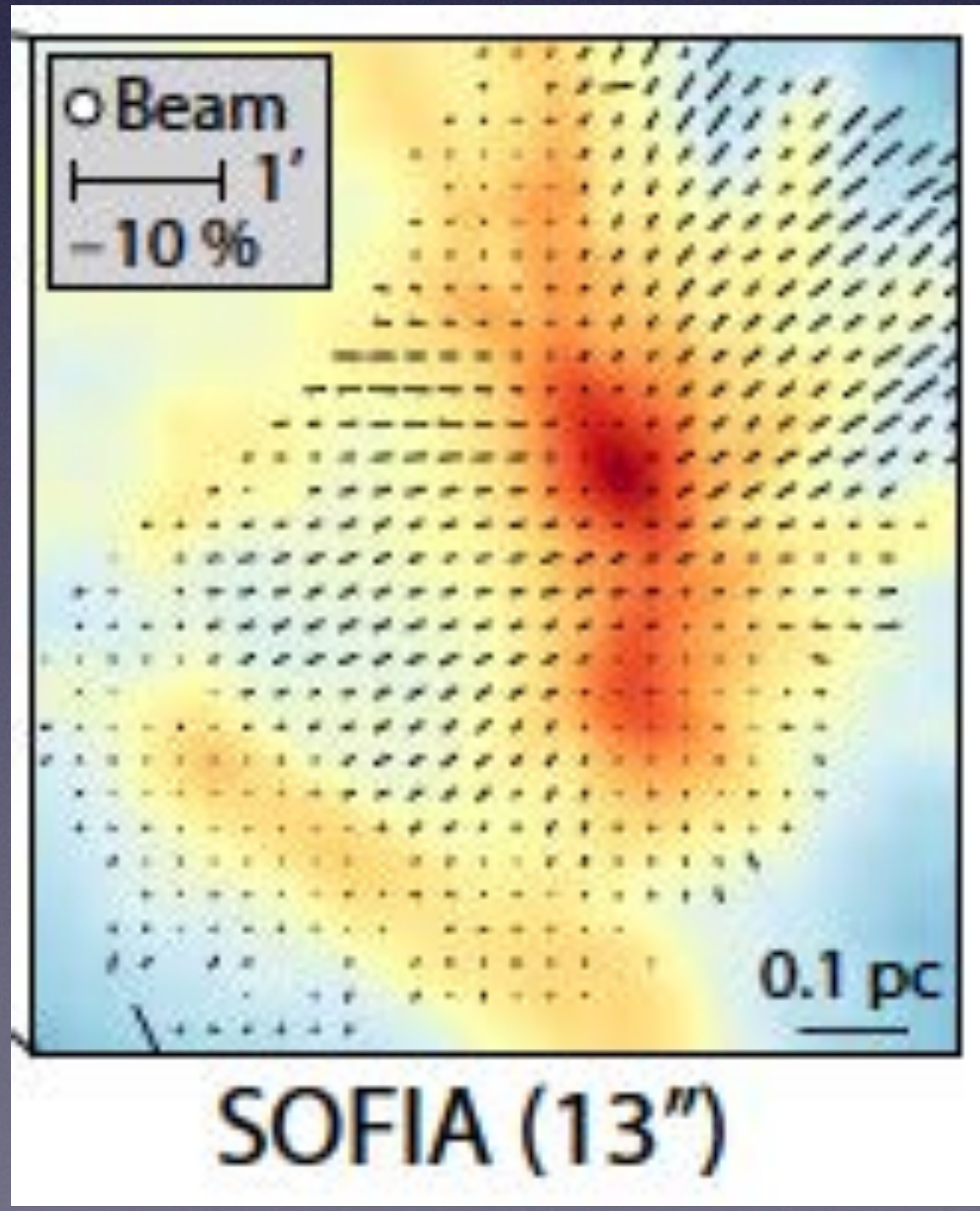

PICO Science : σ_8 - Amplitude of Matter Fluctuations

- Correlations of lensing map with LSST galaxies

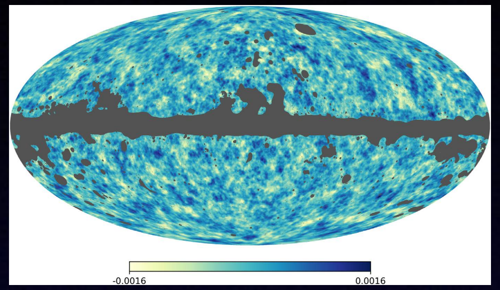

x

- Sub-percent accuracy in each red-shift bin
- 150,000 PICO clusters + redshifts from optical and IR surveys (+ internal mass calibration)
- Sub-percent accuracy for 0.5<z<2
- Determine dark energy parameters, constrain modified gravity, determine neutrino mass

N

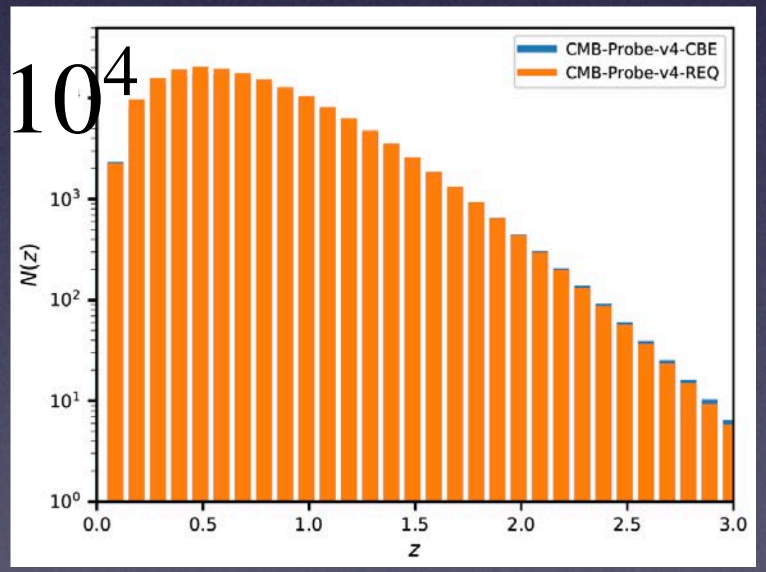

z 3

σ_8 error as a function of L_{max}

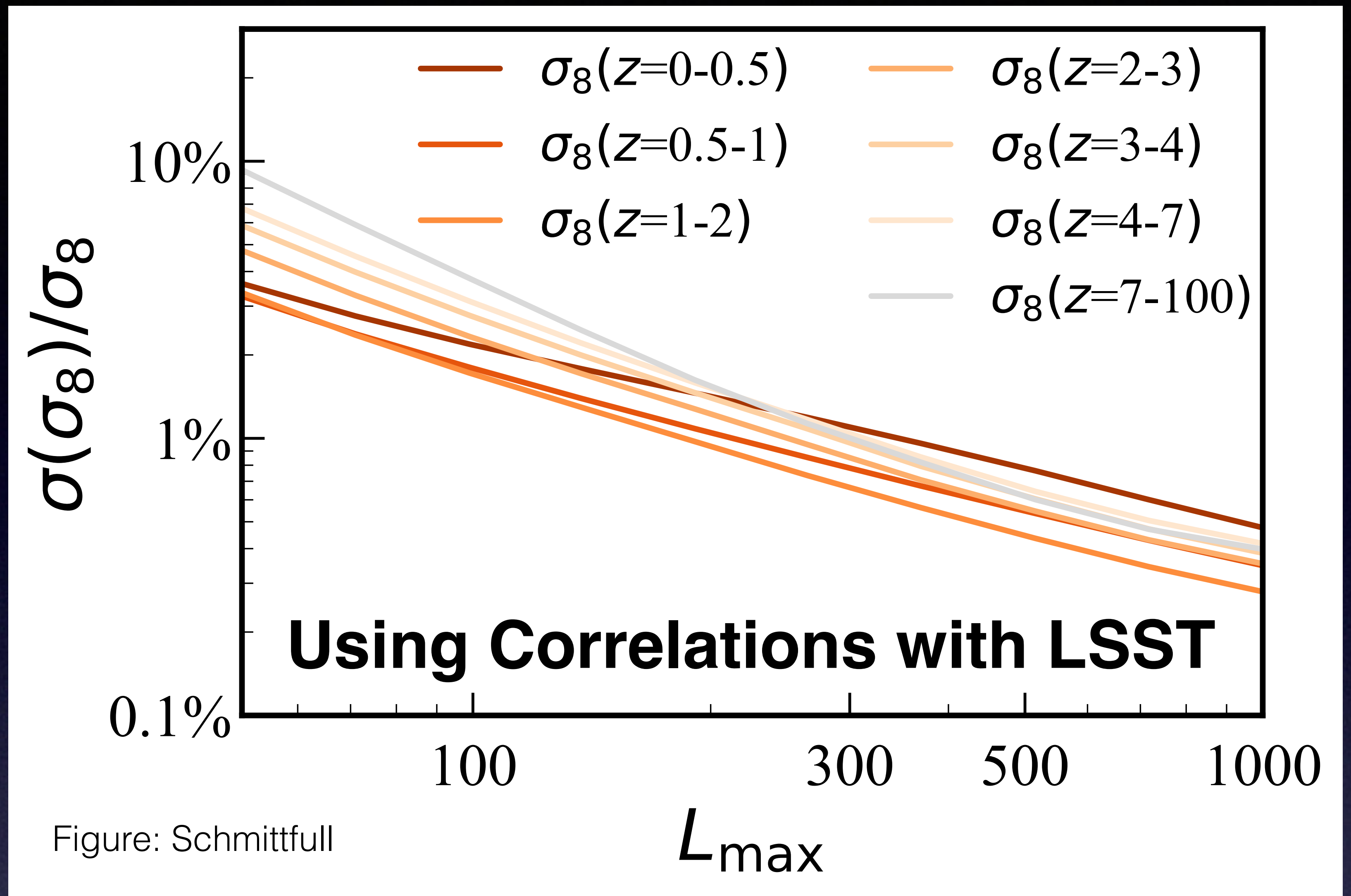

Figure: Schmittfull

σ_8 error vs redshift

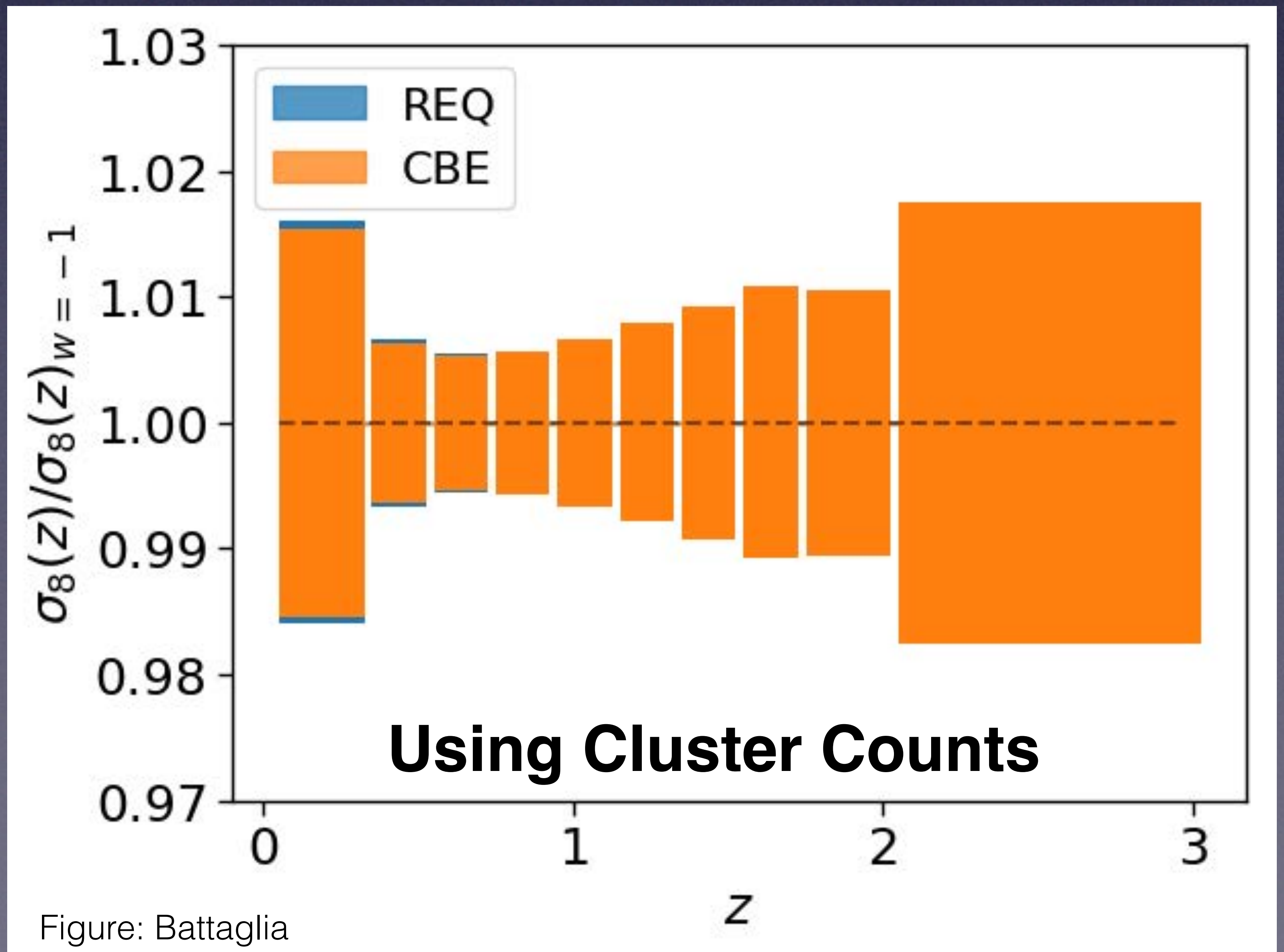

Figure: Battaglia

PICO Science : tSZ Compton-y map

- tSZ: scattering of CMB from hot cluster electrons => integrated electron pressure along line of sight
- PICO 21 frequency bands enable signal separation to give thermal SZ signature over the sky
- SNR for yy spectrum is ~x100 higher than Planck
- SNR = 3000 for cross-correlations with LSST gold weak lensing sample
- Will breakdown correlations to tomographic redshift bins to track evolution of electron pressure with z => constrain the role of energetic feedback in structure formation

Compton-y power spectrum

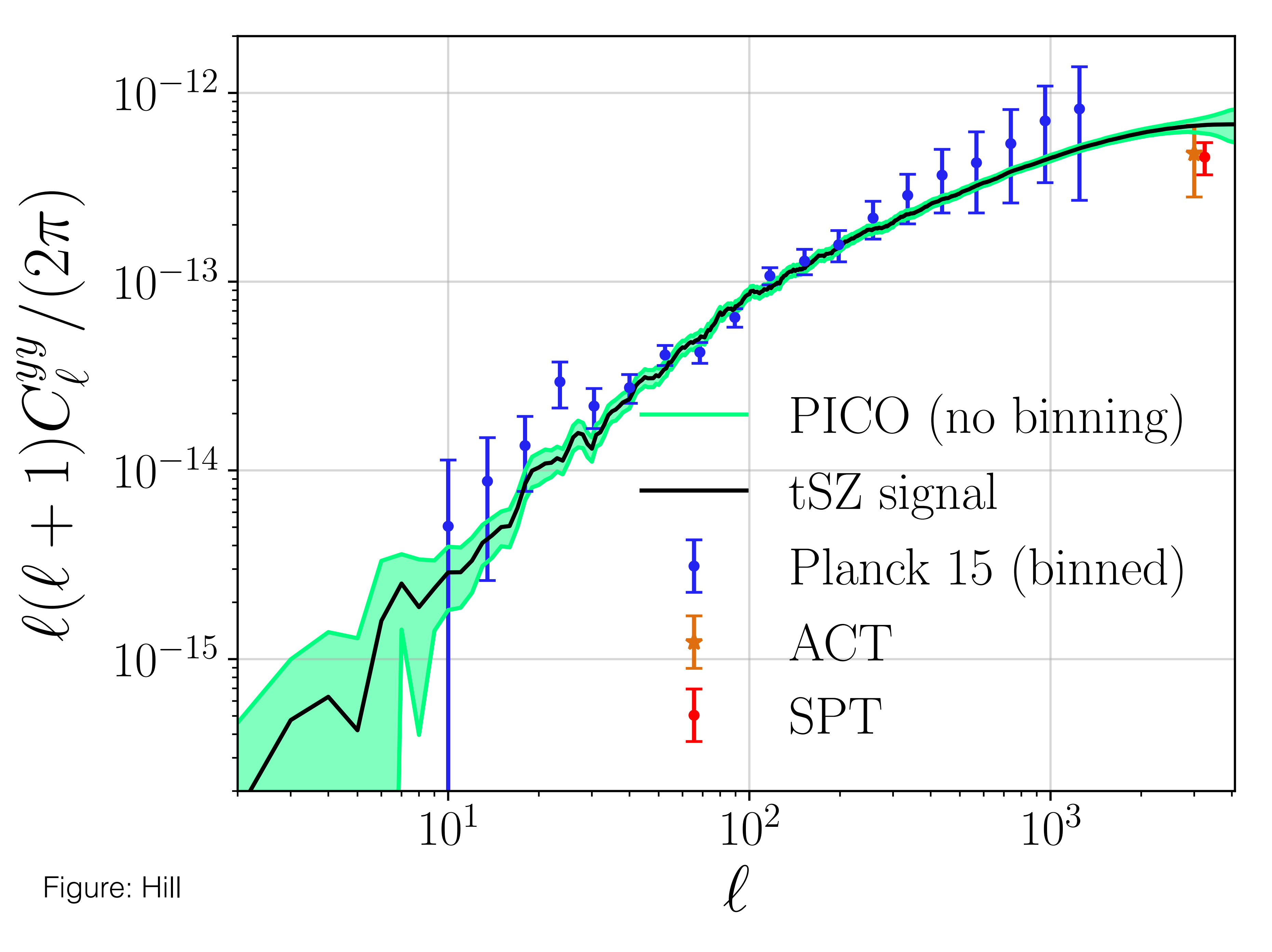

PICO Science : Legacy Surveys

- 4500 strongly lensed galaxies, z~5; early galaxy formation (currently 13)
- 50,000 proto-clusters, z~4.5; early cluster formation (currently few tens)
- 30,000 galaxies, z<0.1; dust SED vs galaxy properties (currently 3400 candidates)
- 2000 polarized radio sources; physics of jets (currently 200)
- Polarization of few thousand dusty galaxies; ordering of magnetic fields in external galaxies

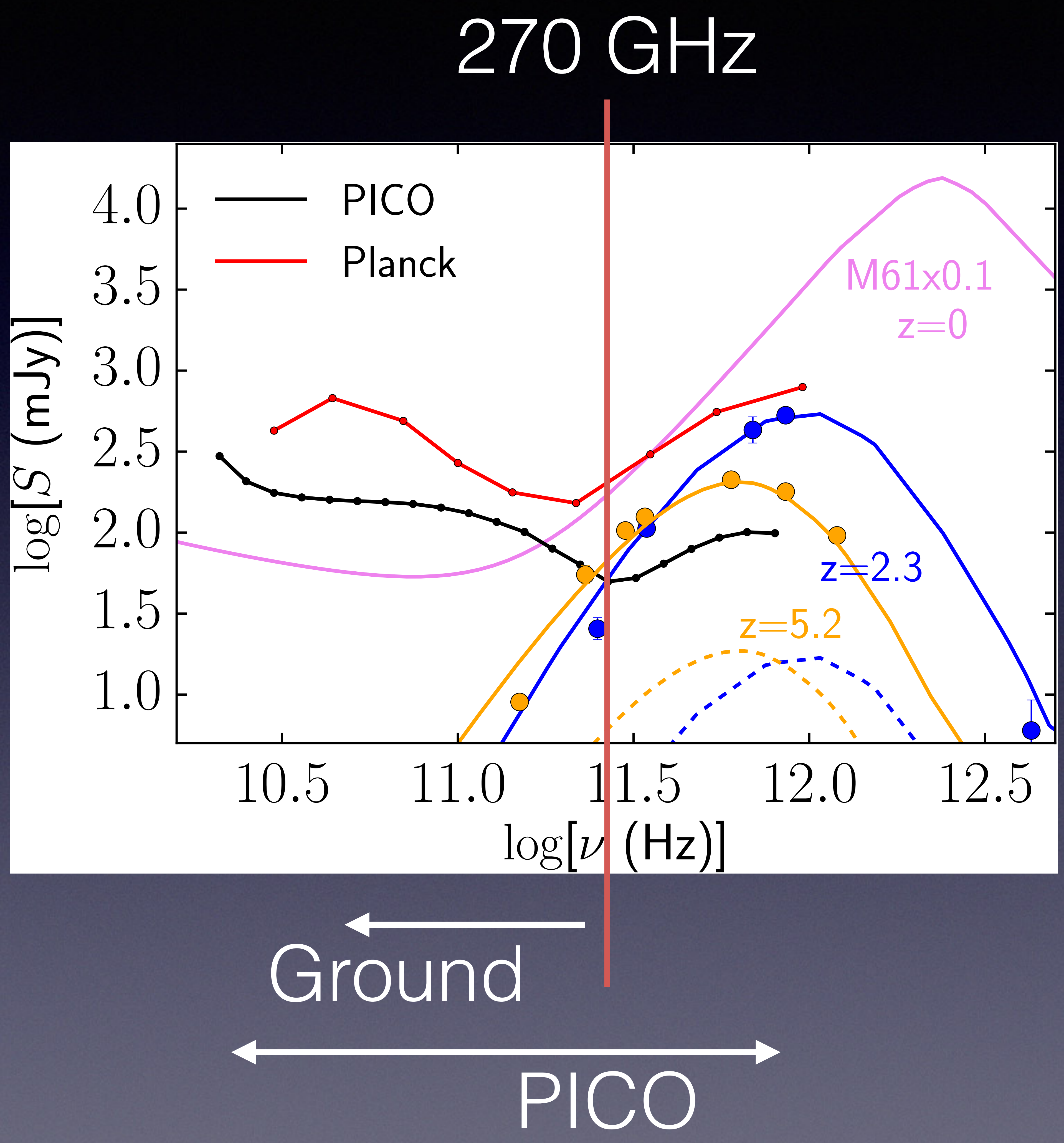

Discovery Space : is ΛCDM Correct?

- ΛCDM gives good fit to data with 6 parameters

- But with not-well-understood universe

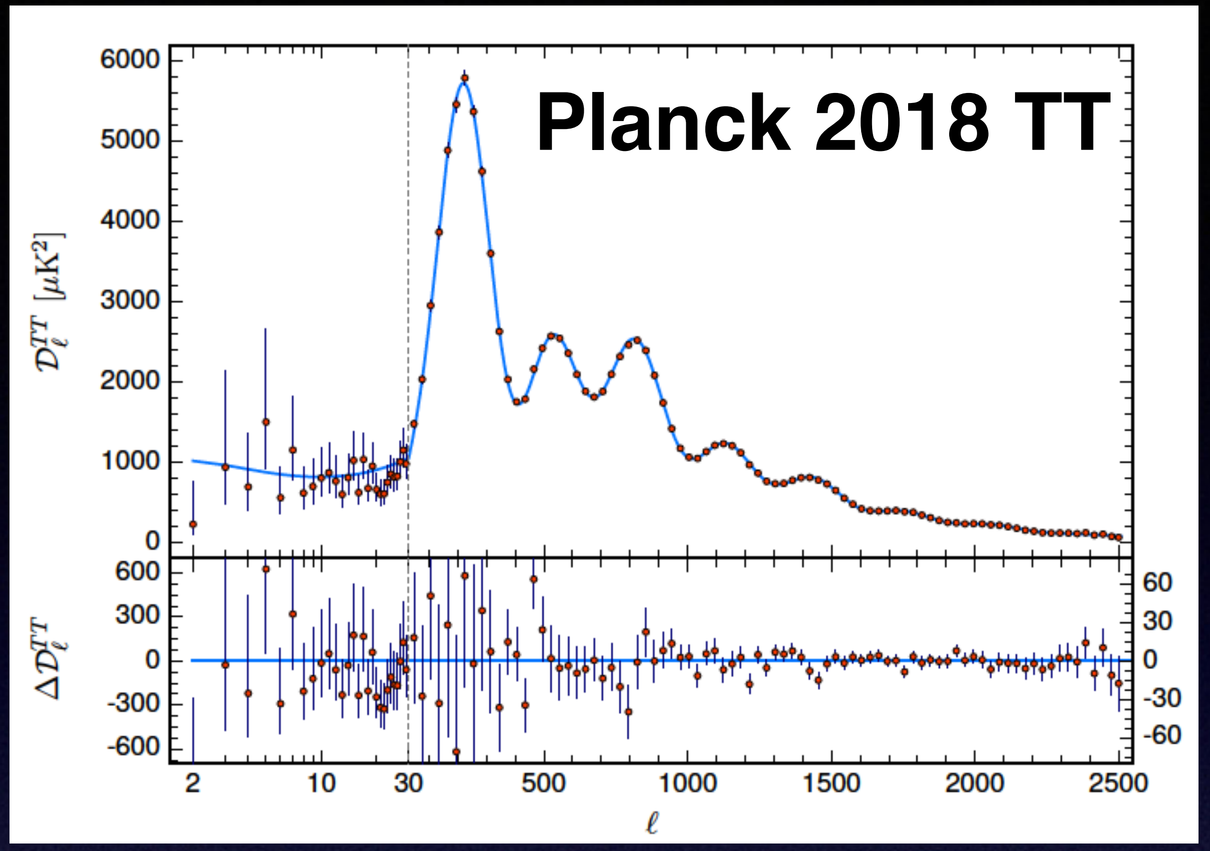

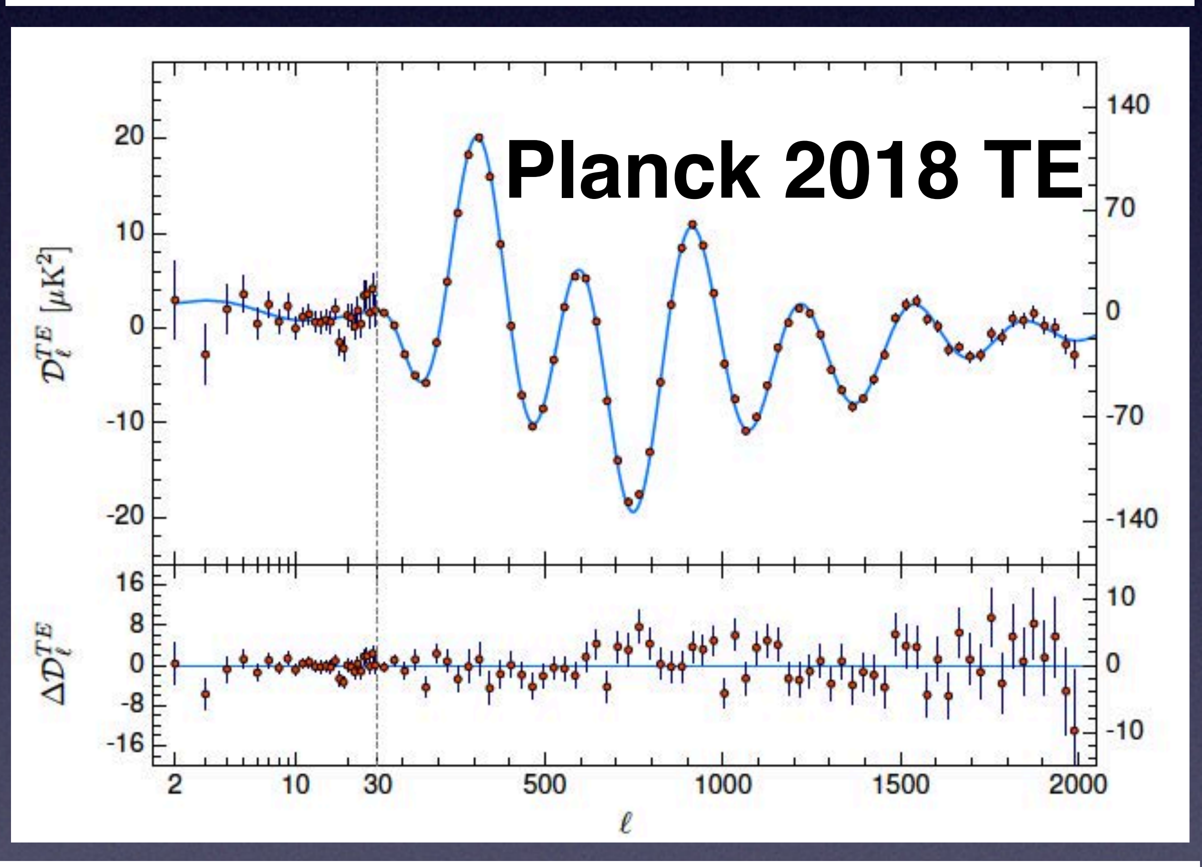

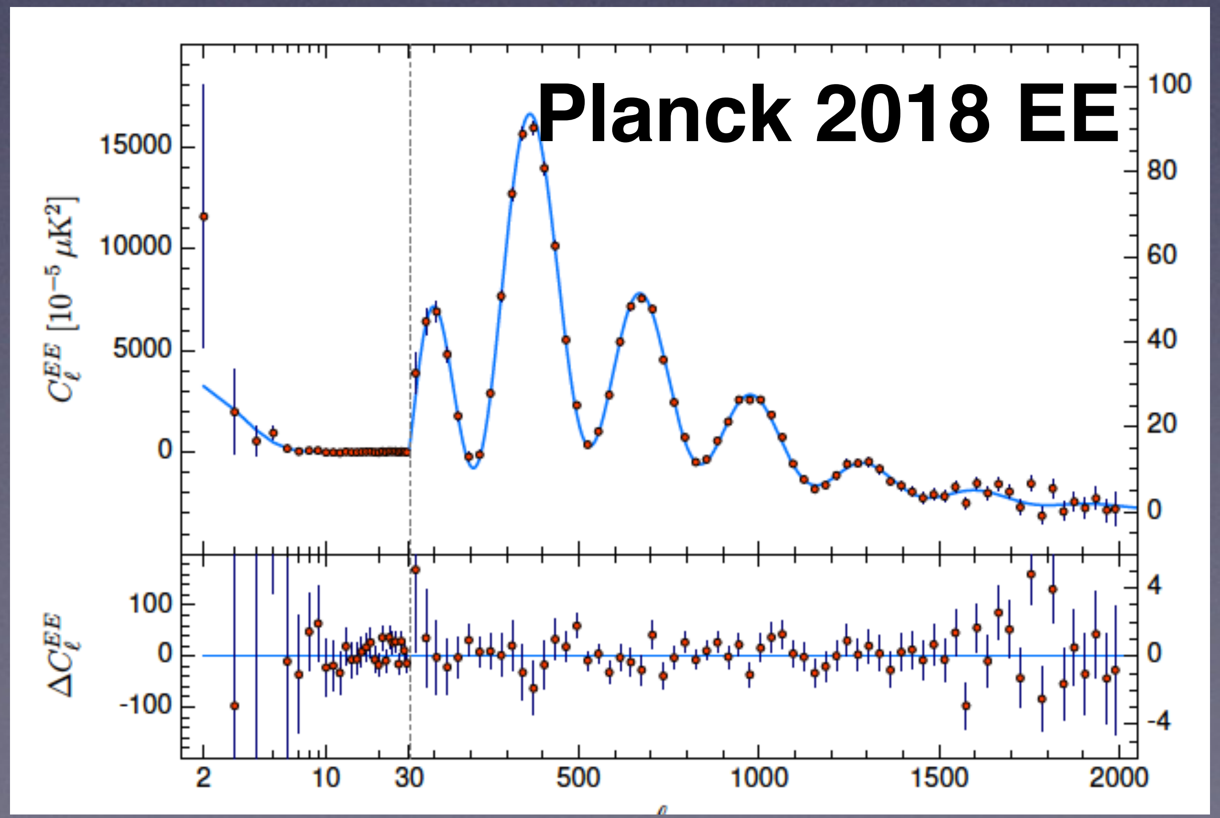

Discovery Space : is ΛCDM Correct?

- ΛCDM gives good fit to data with 6 parameters
- But with not-well-understood universe
- And outstanding puzzles
  - 3.6σ discrepancy with local universe H_0
  - 0.1% probability for low power in TT
  - σ_8 tension(?) between Planck spectra and cosmic shear surveys

H_0

Planck: 67.4 ± 0.5 Planck 2018

SHOES: 73.5 ±1.6 Riess+ 2018

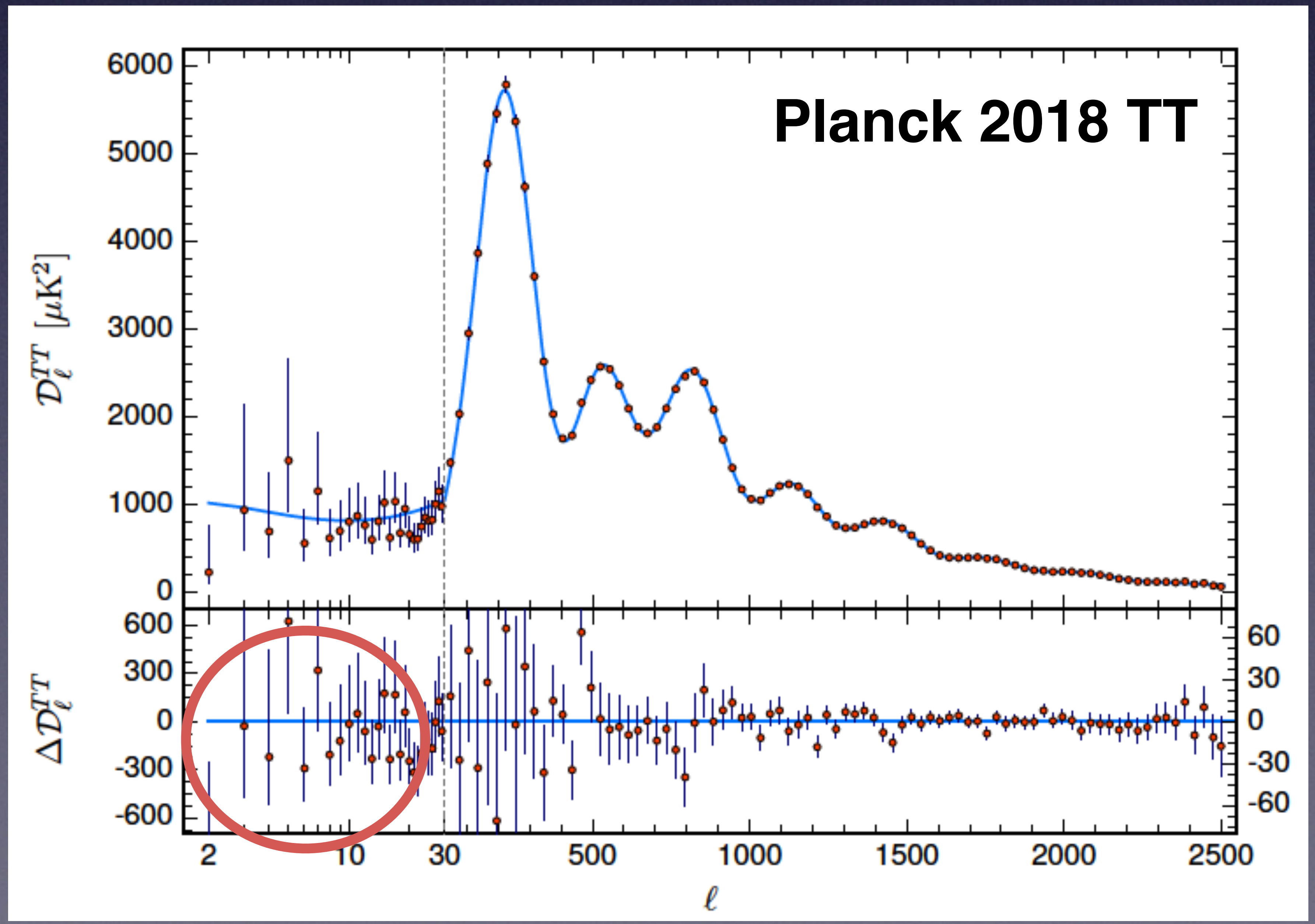

PICO Science : is ΛCDM Correct?

- Compare volume of uncertainty in parameter space relative to Planck
- 1/volume $\propto$ FOM = $\left(\det\left(\mathrm{cov}[p_i]\right)\right)^{-1/2}$

Current Estimate: PICO v4.0 — Baseline: PICO v4.1

	Model	PICO v4.0	PICO v4.1	Planck18
11 parameters	ΛCDM $+ N_{\rm eff} + \alpha_1 + w_0 + w_a + \Sigma m_\nu$	7.4×10^6	4.8×10^6	1
12 parameters	ΛCDM $+ N_{\rm eff} + \alpha_1 + w_0 + w_a + r + \Sigma m_\nu$	2.7×10^{10}	9.5×10^9	1

Di Valentino

Discovery Space : Primordial Magnetic Fields + Birefringence

- Were there primordial magnetic fields?
  - Some young galaxies show magnetic fields that are too strong to be explained by simple dynamo effect
- PICO: B<0.1 nG (1σ) => rule out purely primordial origin of the largest observed B fields {Through Faraday rotation / EB, TB correlations}
- Extensions to standard model have parity violating particles in the early universe => cosmic birefringence => EB, TB correlations
- PICO: x300 improvement in constraints on rotation due to birefringence

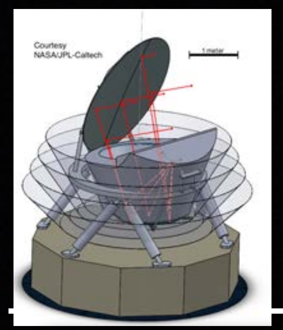

PICO Implementation

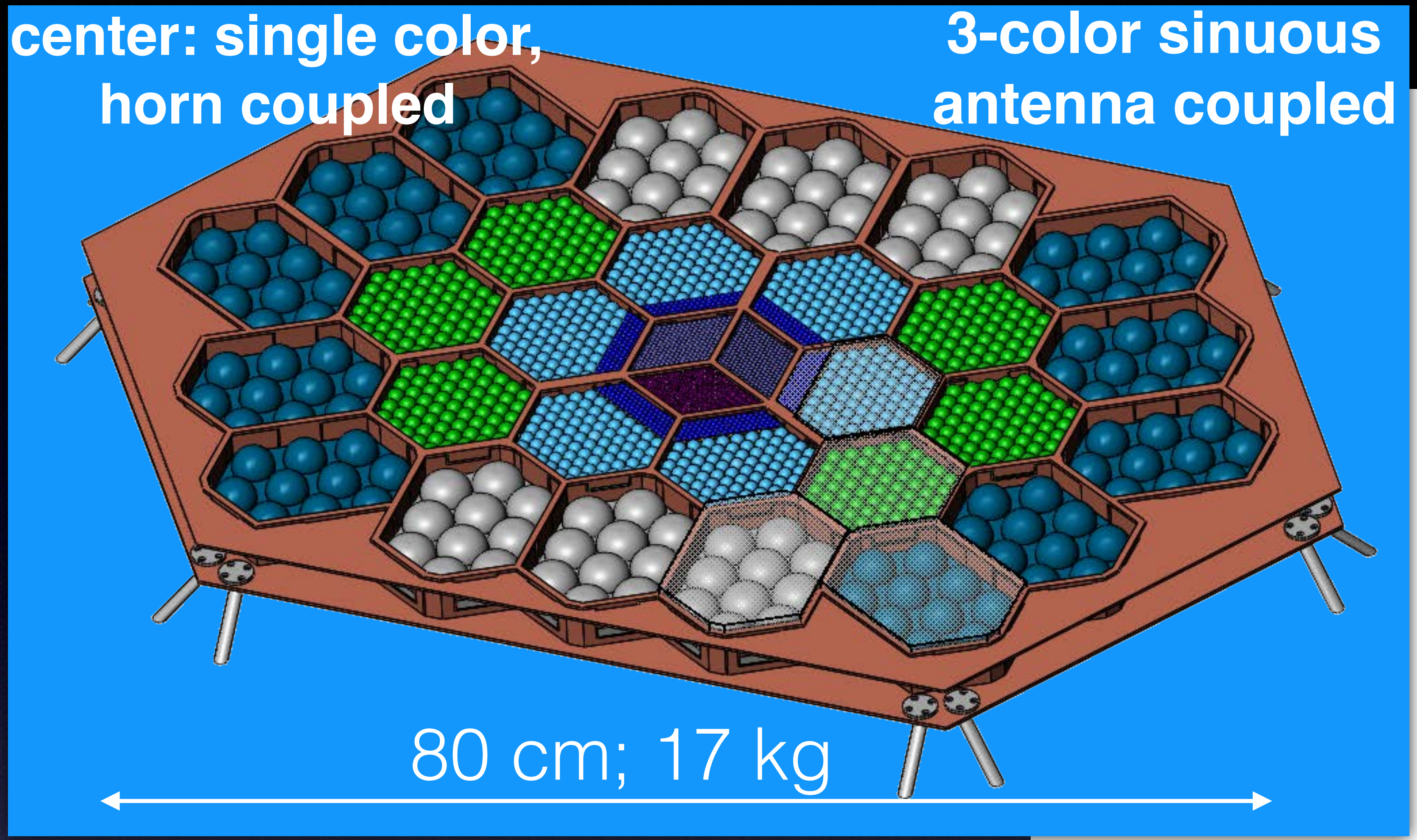

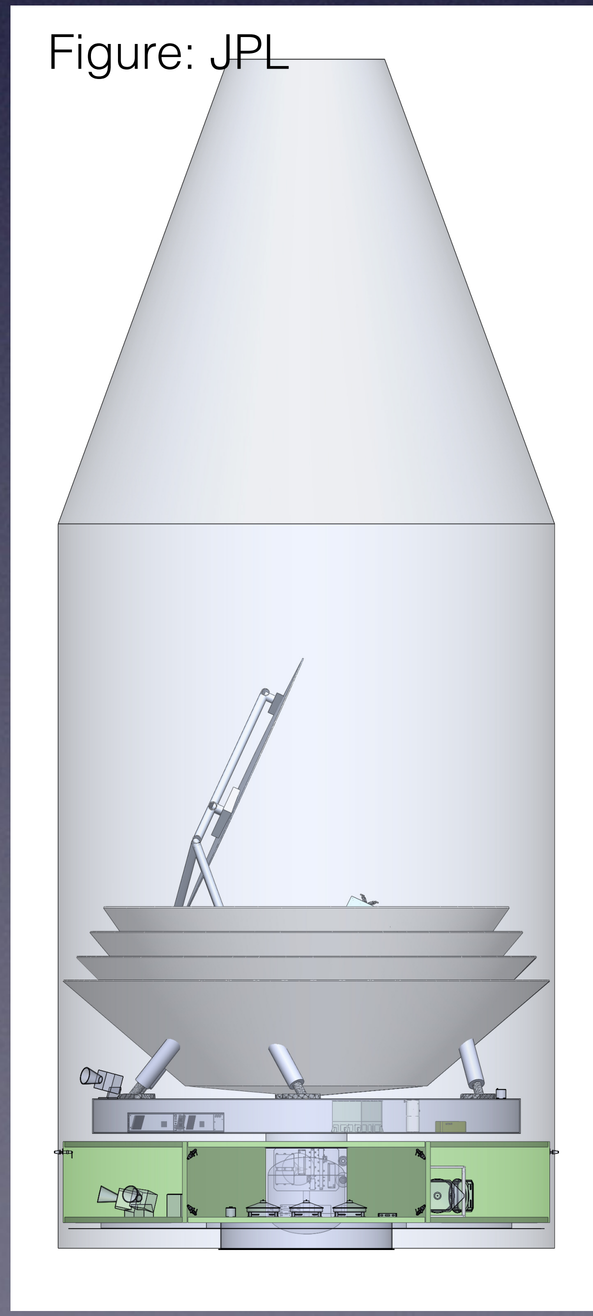

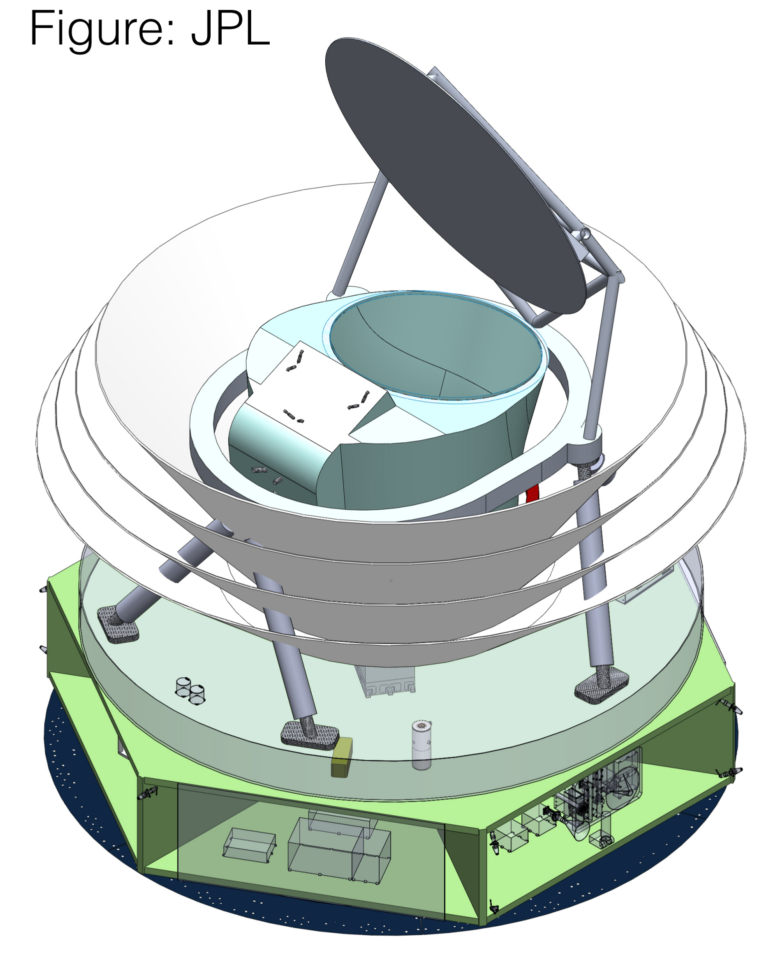

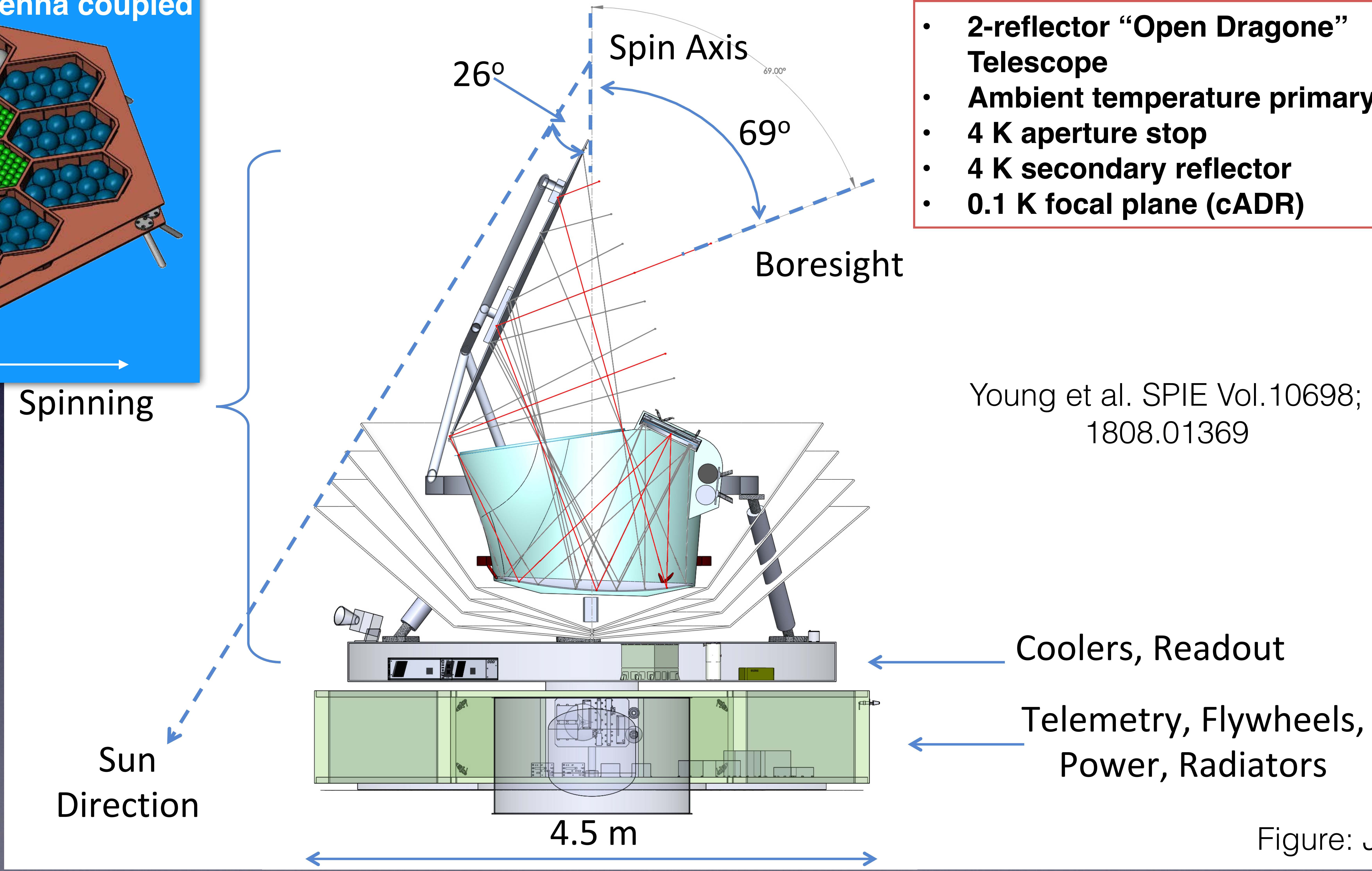

- **2-reflector "Open Dragone" Telescope**
- **Ambient temperature primary**
- **4 K aperture stop**
- **4 K secondary reflector**
- **0.1 K focal plane (cADR)**

Young et al. SPIE Vol.10698;
1808.01369

Figure: JPL

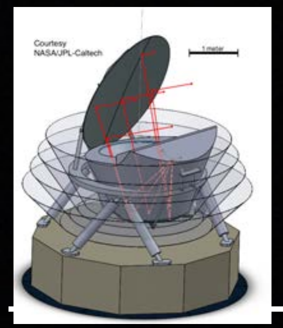

PICO Implementation

Dipole Signal Magnitude over 1 year

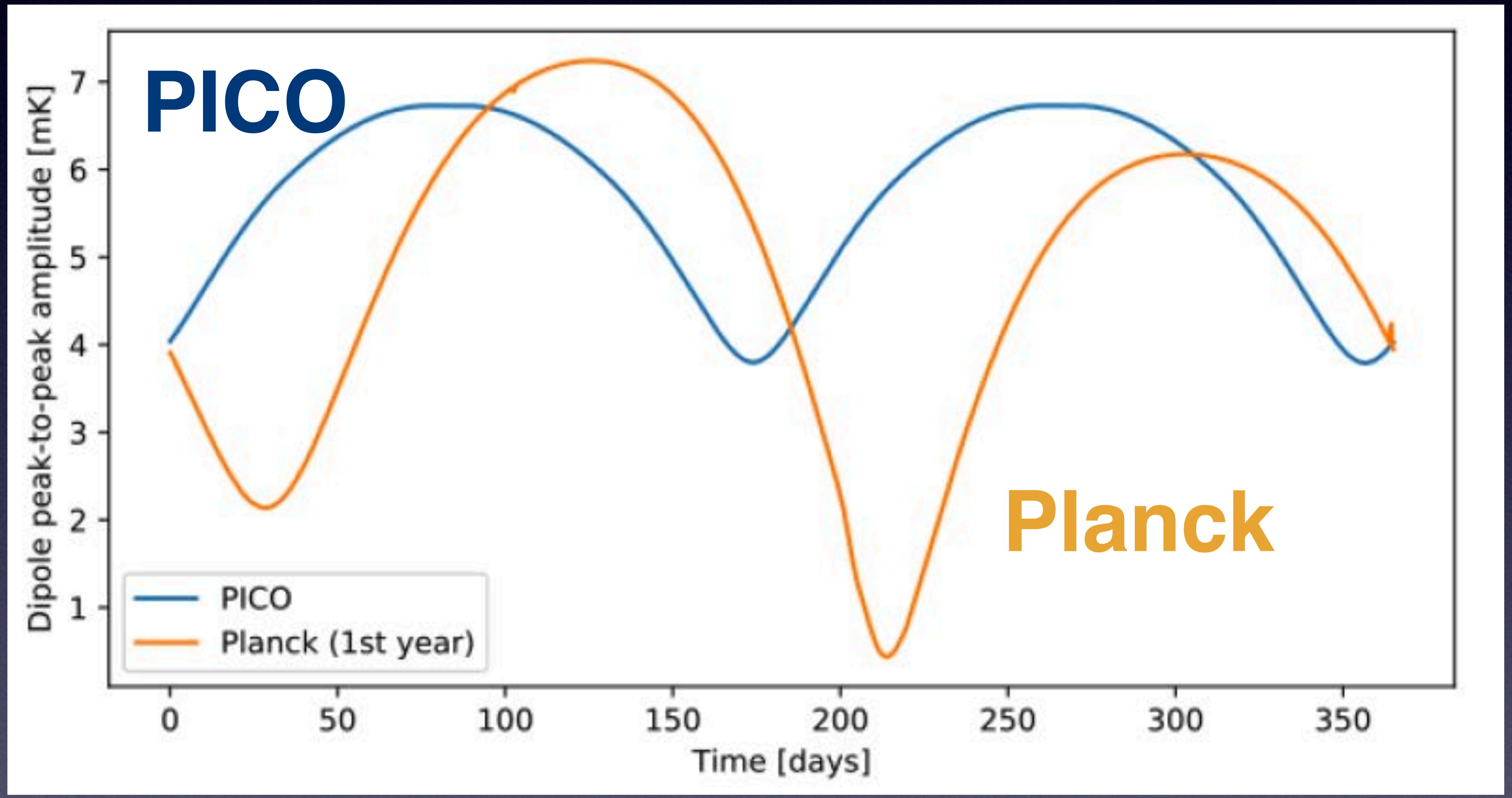

signals are always > 4 mK

- Orbit: L2
- Spinning instrument, static bus
- Spin: 1 rpm; Precess: 10 hours
- 50% sky coverage in two weeks
- Full sky in 6 months
- All 12,996 detectors will make independent T, Q, U maps

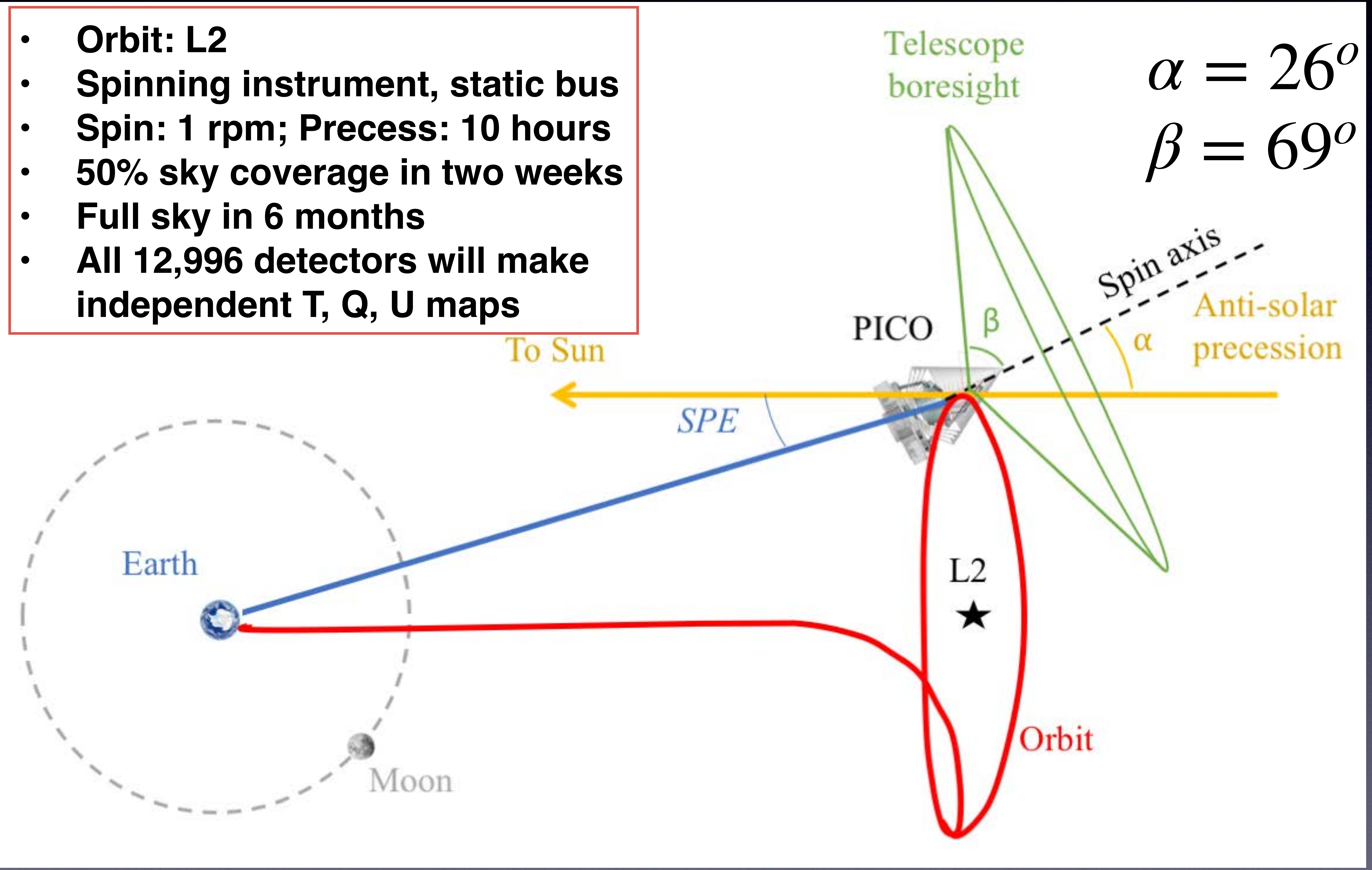

Foreground Removal

- Top Right: PySM model a2d4s1f3; Full sky; nside=512; analyzed with GNILC; 50% of sky; using PICO bands and noise; 85% delensing
- residual foregrounds are x10 below r for \ell=5; x4 below r for ell=100

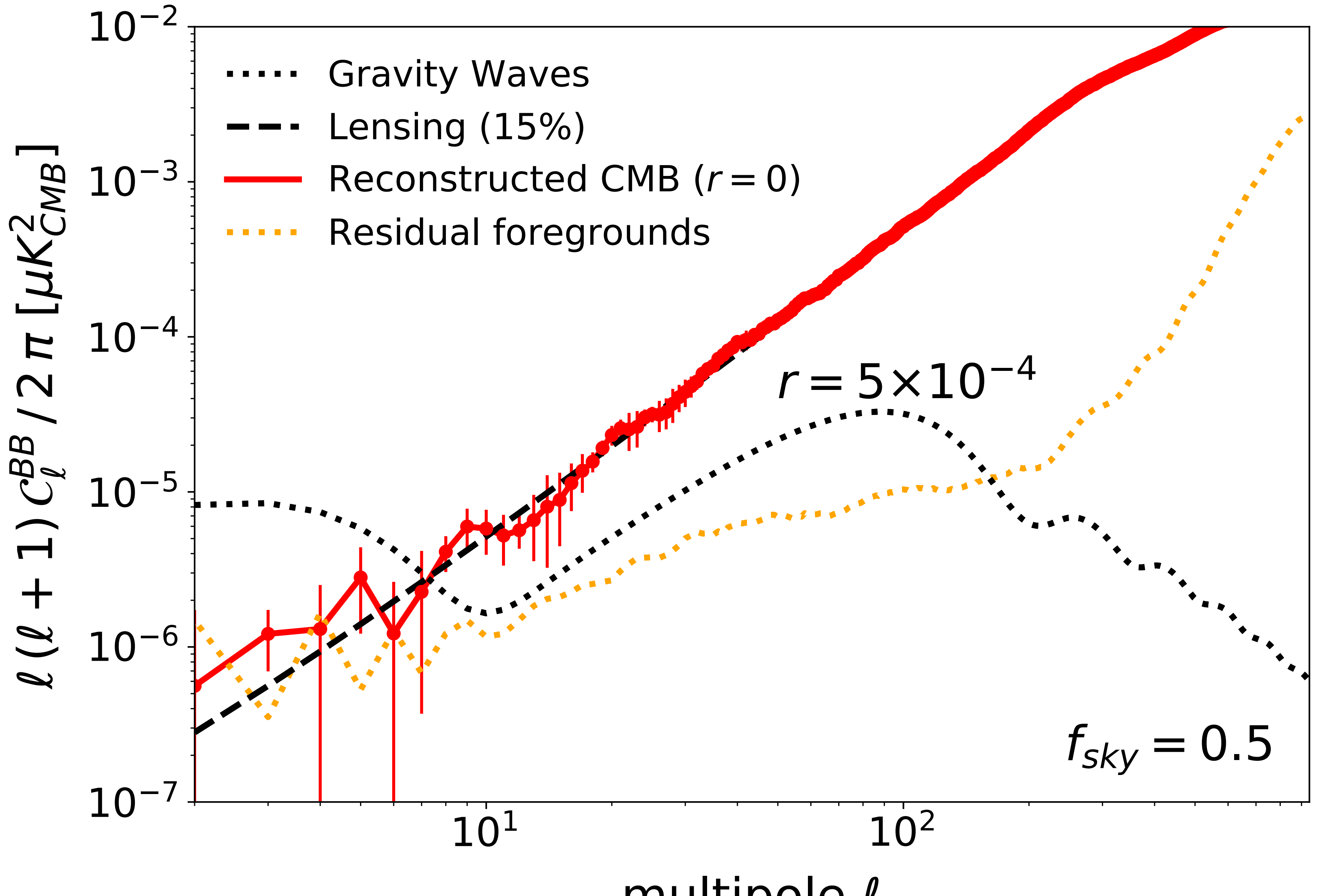

Figure: Remazeilles

- Bottom left: reconstructing CMB and foregrounds with 21 bands has no r bias (r=0.001)
- Bottom right: removing low/high frequencies introduces bias

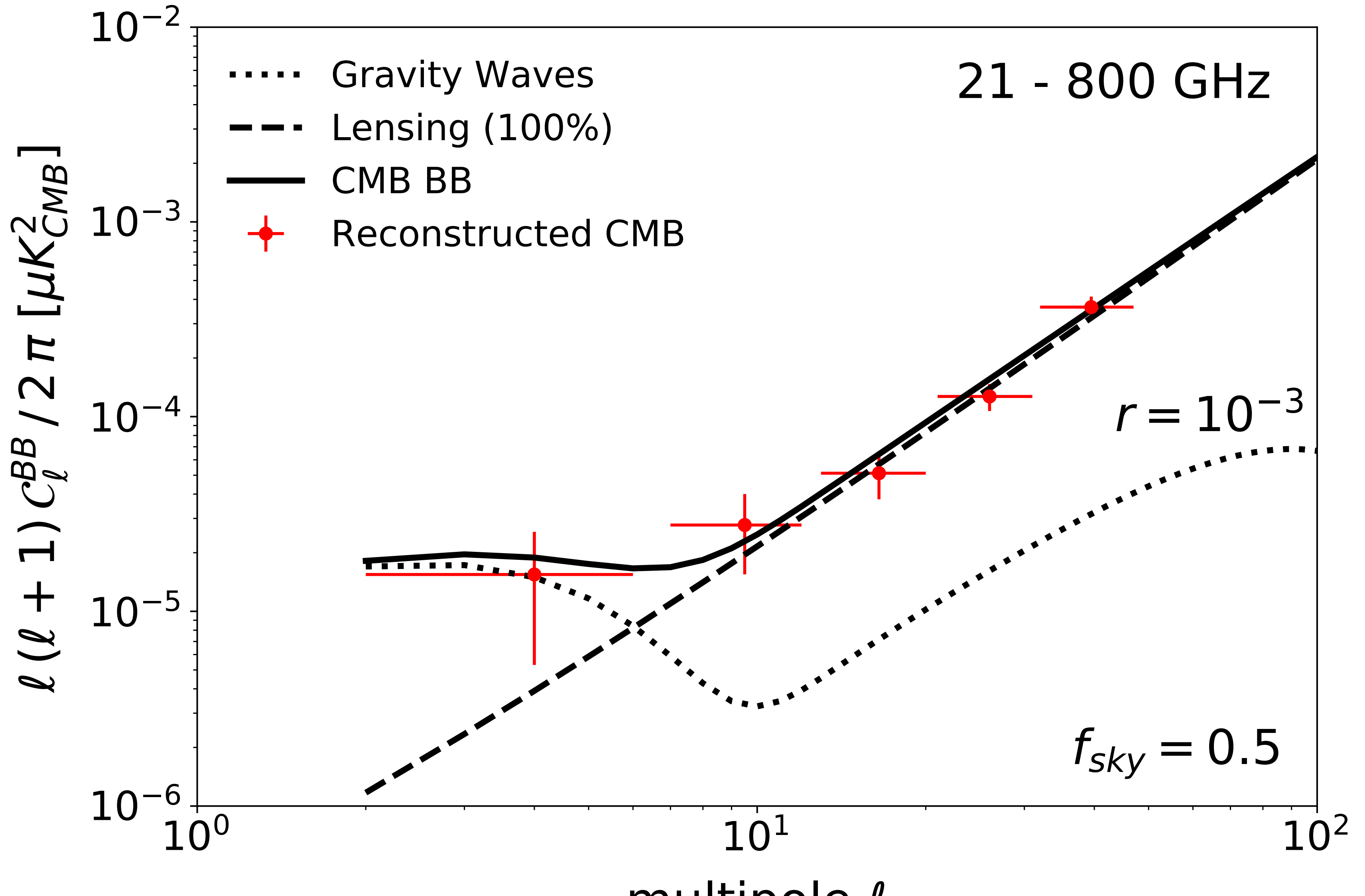

Figure: Remazeilles

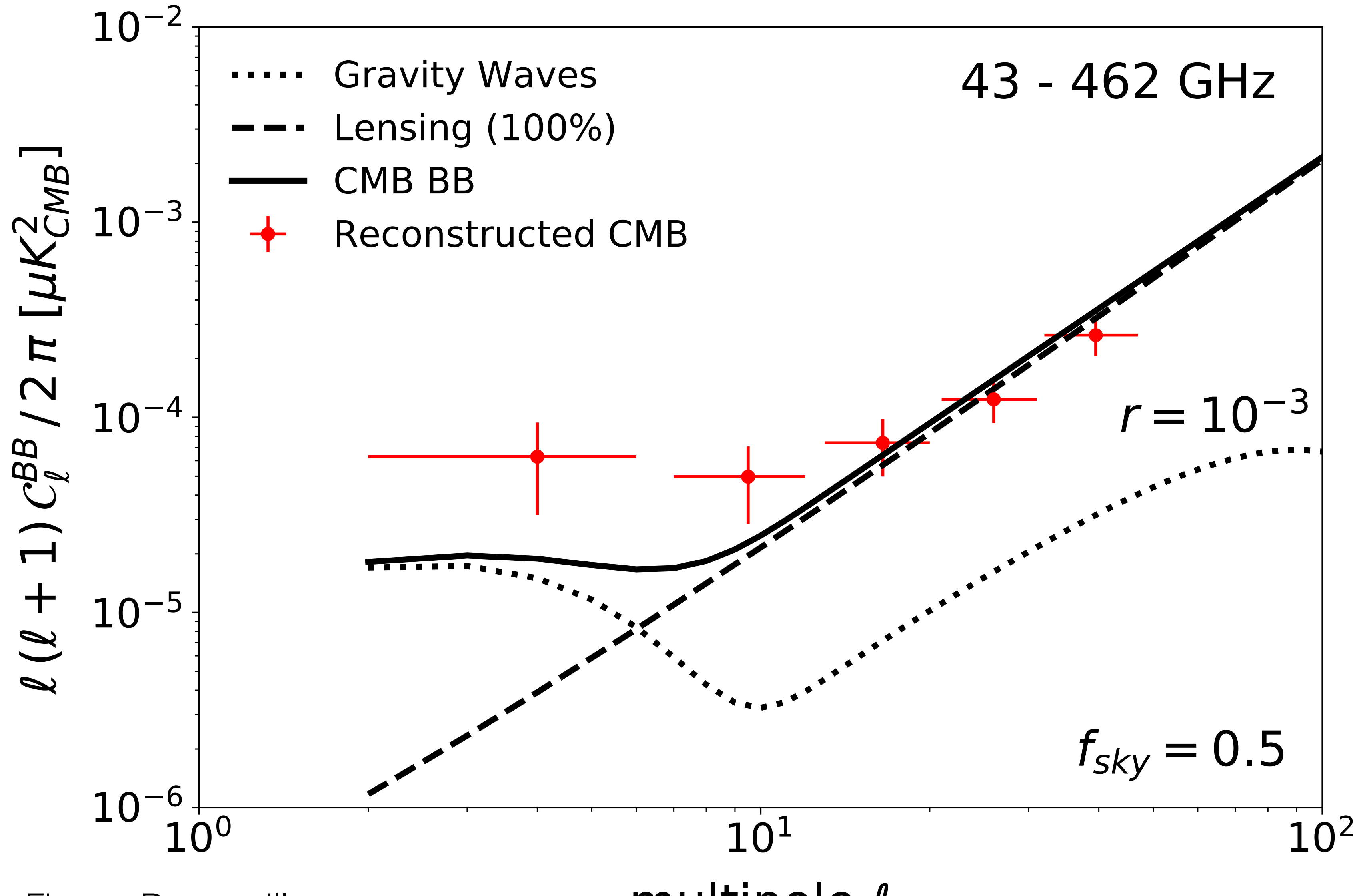

Figure: Remazeilles

Why PICO, Why Now

- PICO is the only instrument with the combination of sky coverage, resolution, frequency bands, and sensitivity to achieve all of the science with one platform.
- Only a space-platform can provide the level of control of systematic uncertainties that PICO will have
  - Each of PICO's 13,000 detectors will make 10 redundant maps of I, Q, U over the entire sky enabling multiple cross-checks and opportunities to identify systematic uncertainties.
  - The thermal environment at L2 is among the most stable available
- Some evidence that PICO has the combination of frequency bands and sensitivity to account for Galactic foregrounds; more verification required
- The implementation relies on current technologies or straightforward extensions
- PICO is the obvious extension to the progress we have made in the last decade.

Figure: R. Flauger

Extra Slides

Inflation - Models that explain n_s

- Models for which $n_s - 1 = -\frac{p+1}{N}$
- N = number of e-folds between the time the pivot scale exits the horizon and the end of inflation
- Mukhanov (2013), Roest (2014), Creminelli+(2015)

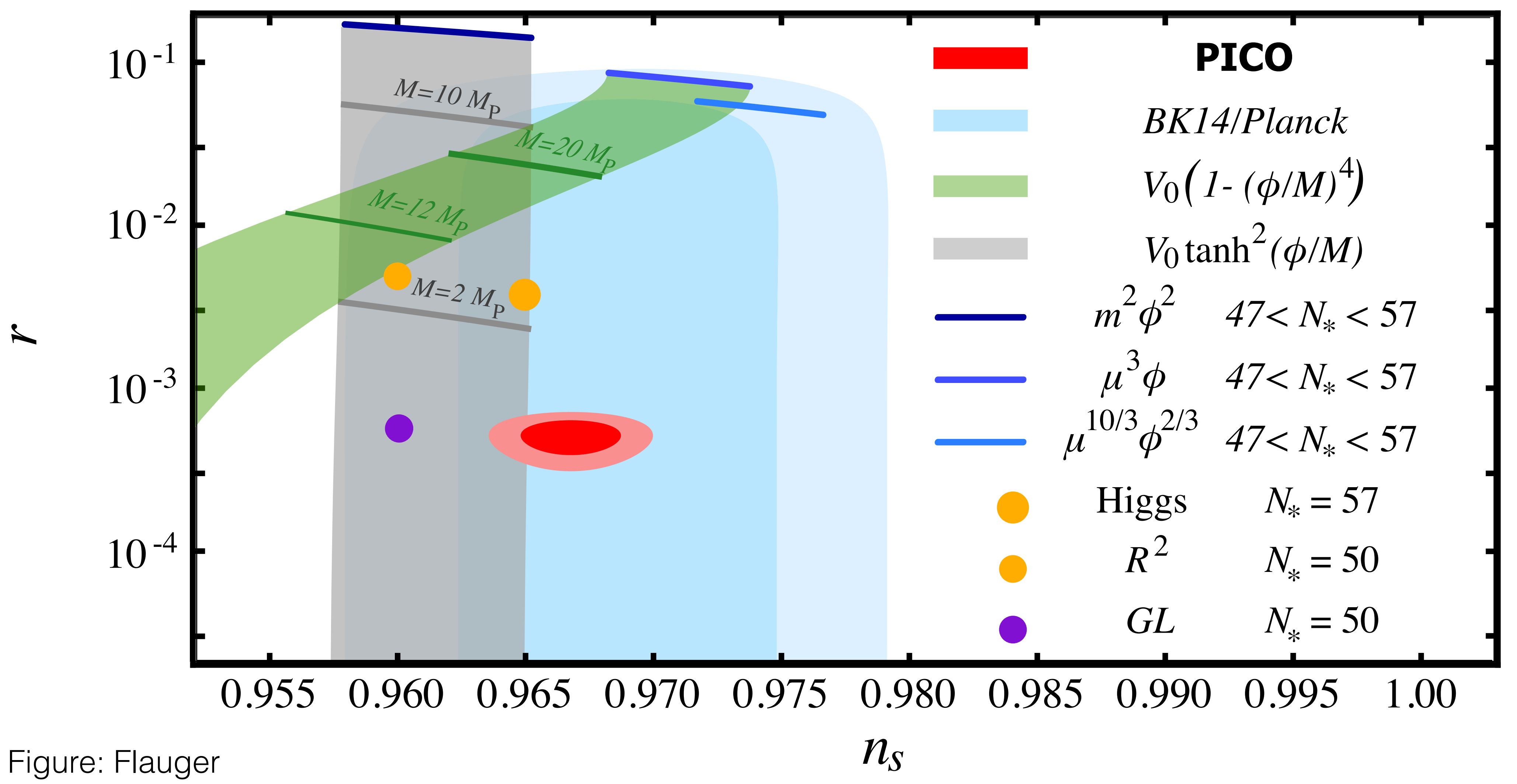

Figure: Flauger

Table 3.2: PICO has 21 partially overlapping frequency bands with band centers (ν_c) from 21 GHz to 799 GHz and each with bandwidth $\Delta\nu/\nu_c = 25\,\%$. The beams are single mode, with FWHM sizes of $6\farcm2 \times (155\,\mathrm{GHz}/\nu_c)$. The CBE per-bolometer sensitivity is photon-noise limited (§ 3.2.3). The total number of bolometers for each band is equal to (number of tiles) × (pixels per tile) × (2 polarizations per pixel), from Table 3.1. Array sensitivity assumes 90 % detector operability. The map depth assumes 5 yr of full sky survey at 95 % survey efficiency, except the 25 and 30 GHz frequency bands, which are conservatively excluded during 4 hr/day Ka-band (26 GHz) telecom periods (§ 4.2).

Band Center [GHz]	Beam FWHM [arcmin]	CBE Bolo NET [$\mu K_{CMB}\,s^{1/2}$]	N_{bolo}	CBE Array NET [$\mu K_{CMB}\,s^{1/2}$]	Baseline Array NET [$\mu K_{CMB}\,s^{1/2}$]	Baseline polarization map depth [μK_{CMB} arcmin]	[Jy sr^{-1}]
21	38.4	112	120	12.0	17.0	23.9	8.3
25	32.0	103	200	8.4	11.9	18.4	10.9
30	28.3	59.4	120	5.7	8.0	12.4	11.8
36	23.6	54.4	200	4.0	5.7	7.9	12.9
43	22.2	41.7	120	4.0	5.6	7.9	19.5
52	18.4	38.4	200	2.8	4.0	5.7	23.8
62	12.8	69.2	732	2.7	3.8	5.4	45.4
75	10.7	65.4	1020	2.1	3.0	4.2	58.3
90	9.5	37.7	732	1.4	2.0	2.8	59.3
108	7.9	36.2	1020	1.1	1.6	2.3	77.3
129	7.4	27.8	732	1.1	1.5	2.1	96.0
155	6.2	27.5	1020	0.9	1.3	1.8	119
186	4.3	70.8	960	2.0	2.8	4.0	433
223	3.6	84.2	900	2.3	3.3	4.5	604
268	3.2	54.8	960	1.5	2.2	3.1	433
321	2.6	77.6	900	2.1	3.0	4.2	578
385	2.5	69.1	960	2.3	3.2	4.5	429
462	2.1	133	900	4.5	6.4	9.1	551
555	1.5	658	440	23.0	32.5	45.8	1580
666	1.3	2210	400	89.0	126	177	2080
799	1.1	10400	360	526	744	1050	2880
Total			12 996	0.43	0.61	0.87	

Calibration and 1/f

217 GHz

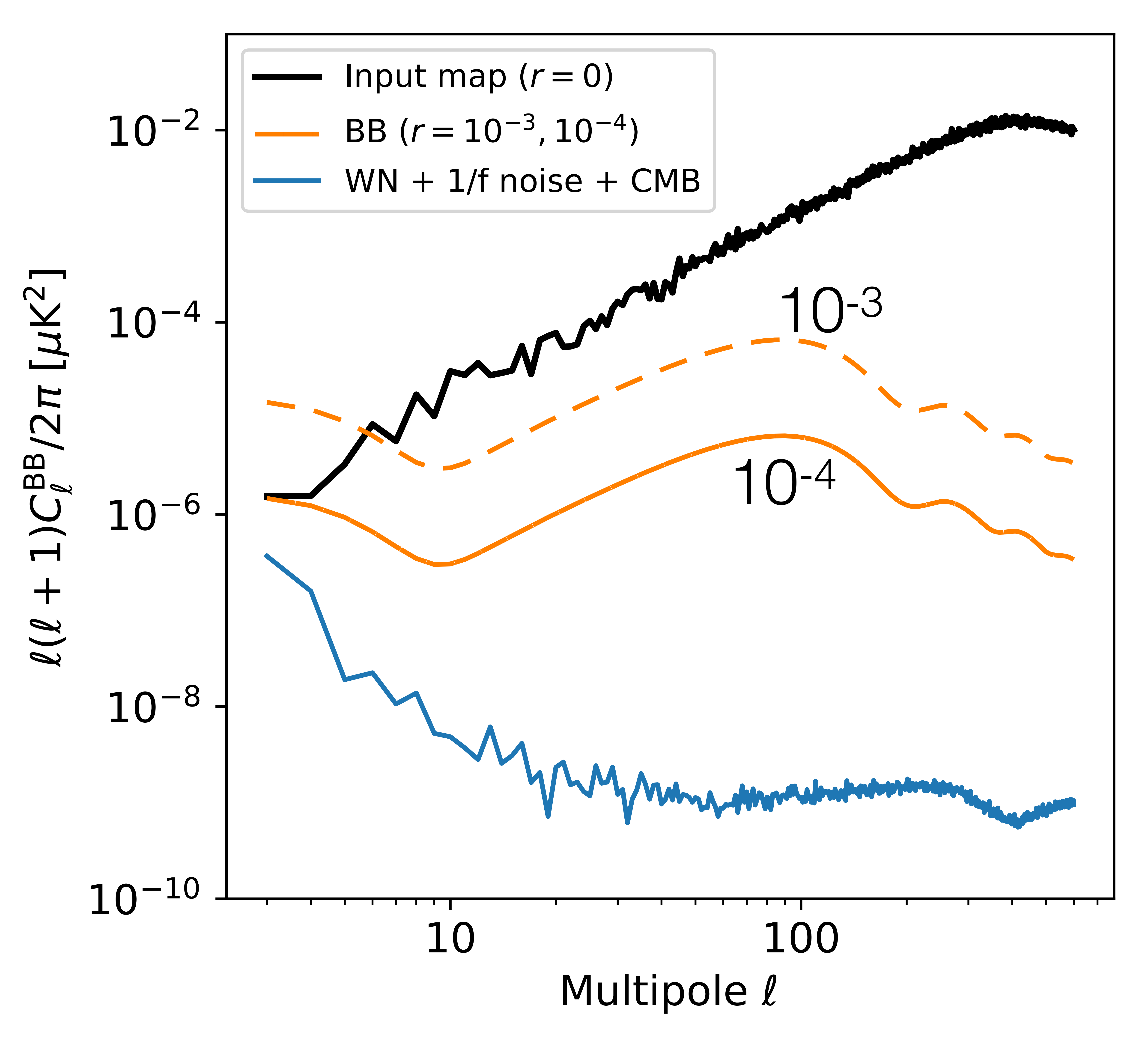

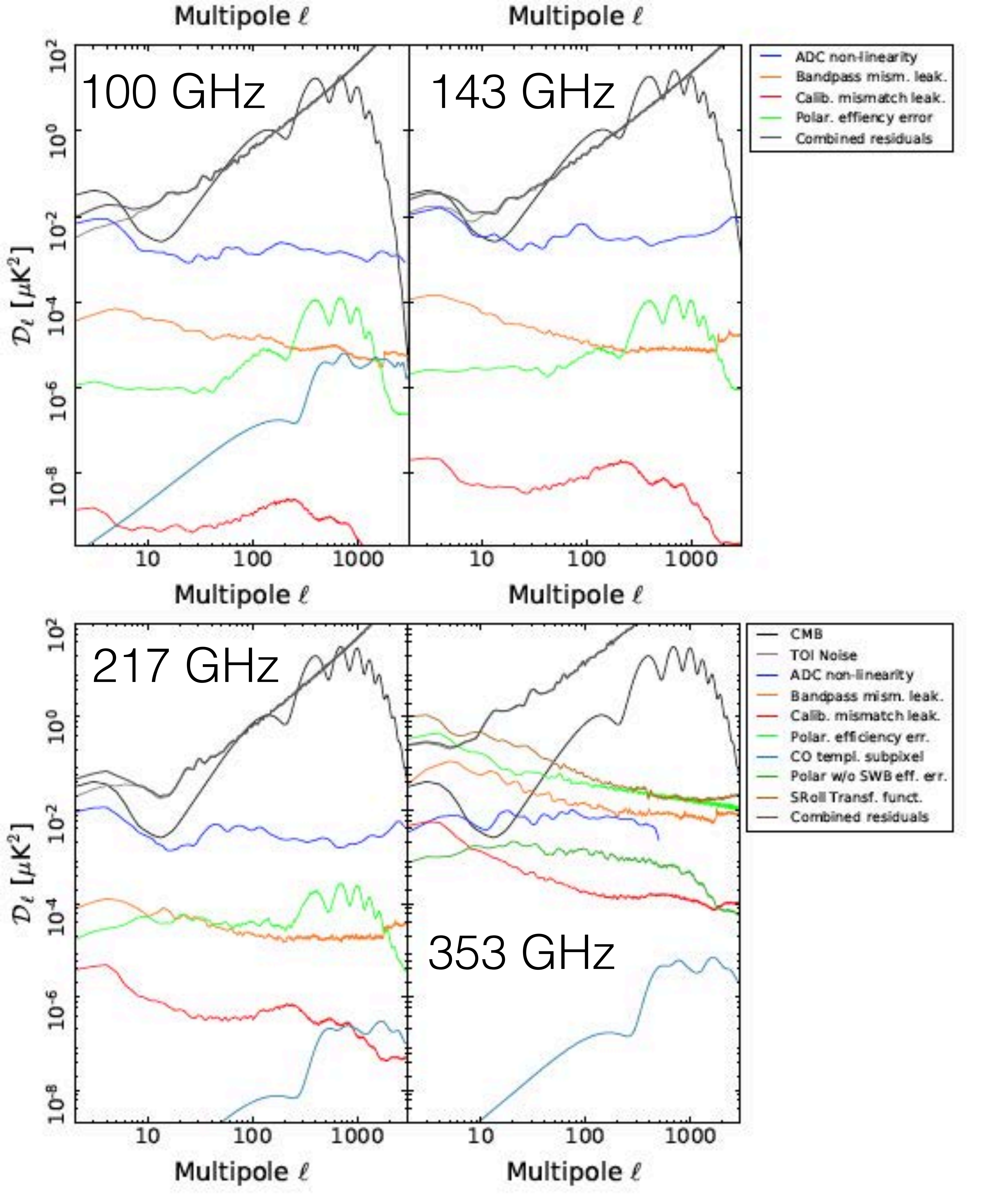
100 GHz
143 GHz
217 GHz
353 GHz
Multipole ℓ
$\mathcal{D}_\ell$ [μK^2]
ADC non-linearity
Bandpass mism. leak.
Calib. mismatch leak.
Polar. effiency error
Combined residuals
CMB
TOI Noise
ADC non-linearity
Bandpass mism. leak.
Calib. mismatch leak.
Polar. efficiency err.
CO templ. subpixel
Polar w/o SWB eff. err.
SRoll Transf. funct.
Combined residuals

30 GHz 70 GHz

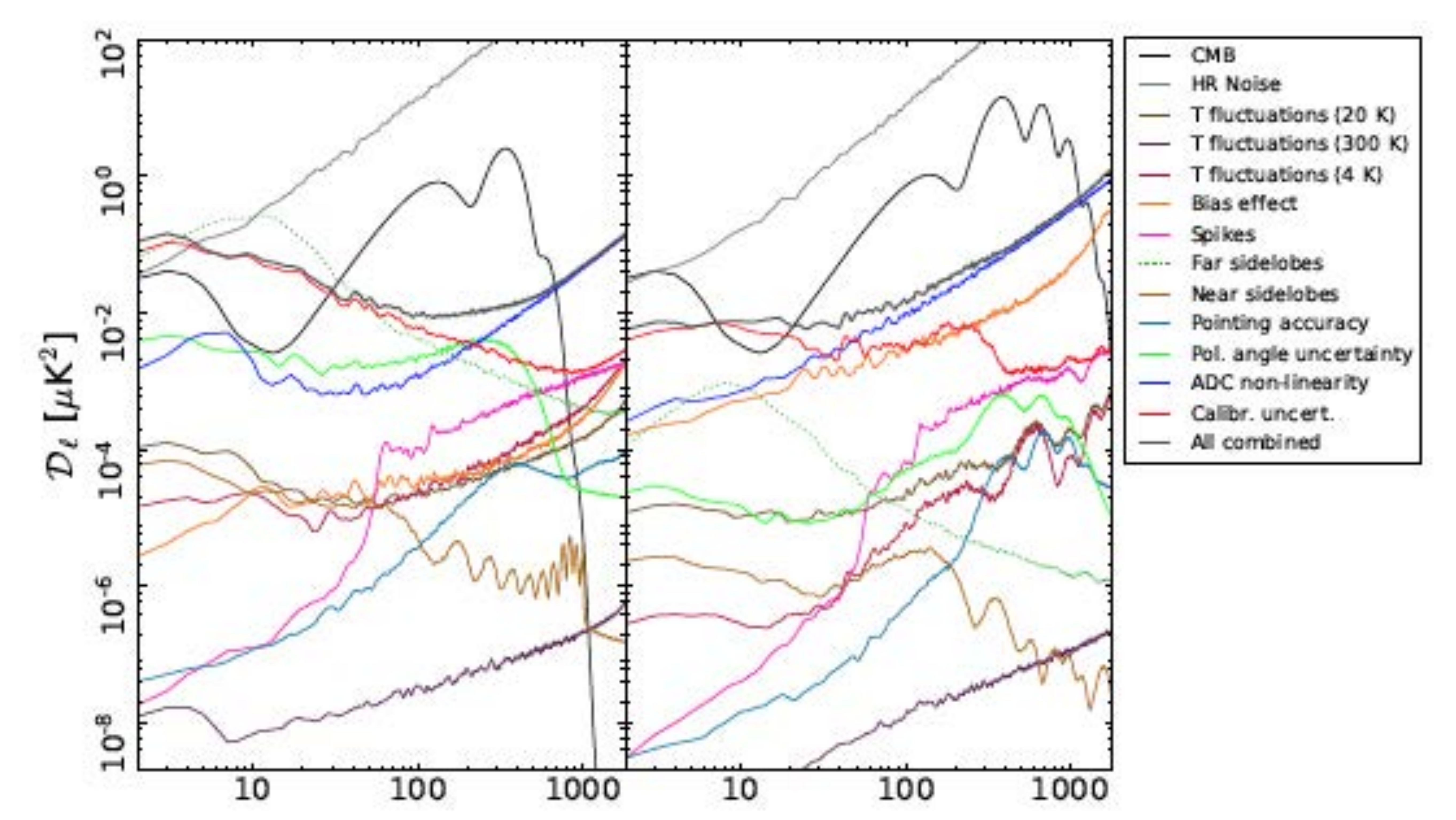
$\mathcal{D}_\ell$ [μK^2]
CMB
HR Noise
T fluctuations (20 K)
T fluctuations (300 K)
T fluctuations (4 K)
Bias effect
Spikes
Far sidelobes
Near sidelobes
Pointing accuracy
Pol. angle uncertainty
ADC non-linearity
Calibr. uncert.
All combined

Foreground Removal

- Top Right: PySM model a2d4s1f3; Full sky; nside=512; analyzed with GNILC; 50% of sky; using PICO bands and noise; 85% delensing
- residual foregrounds are x10 below r for \ell=5; x4 below r for ell=100

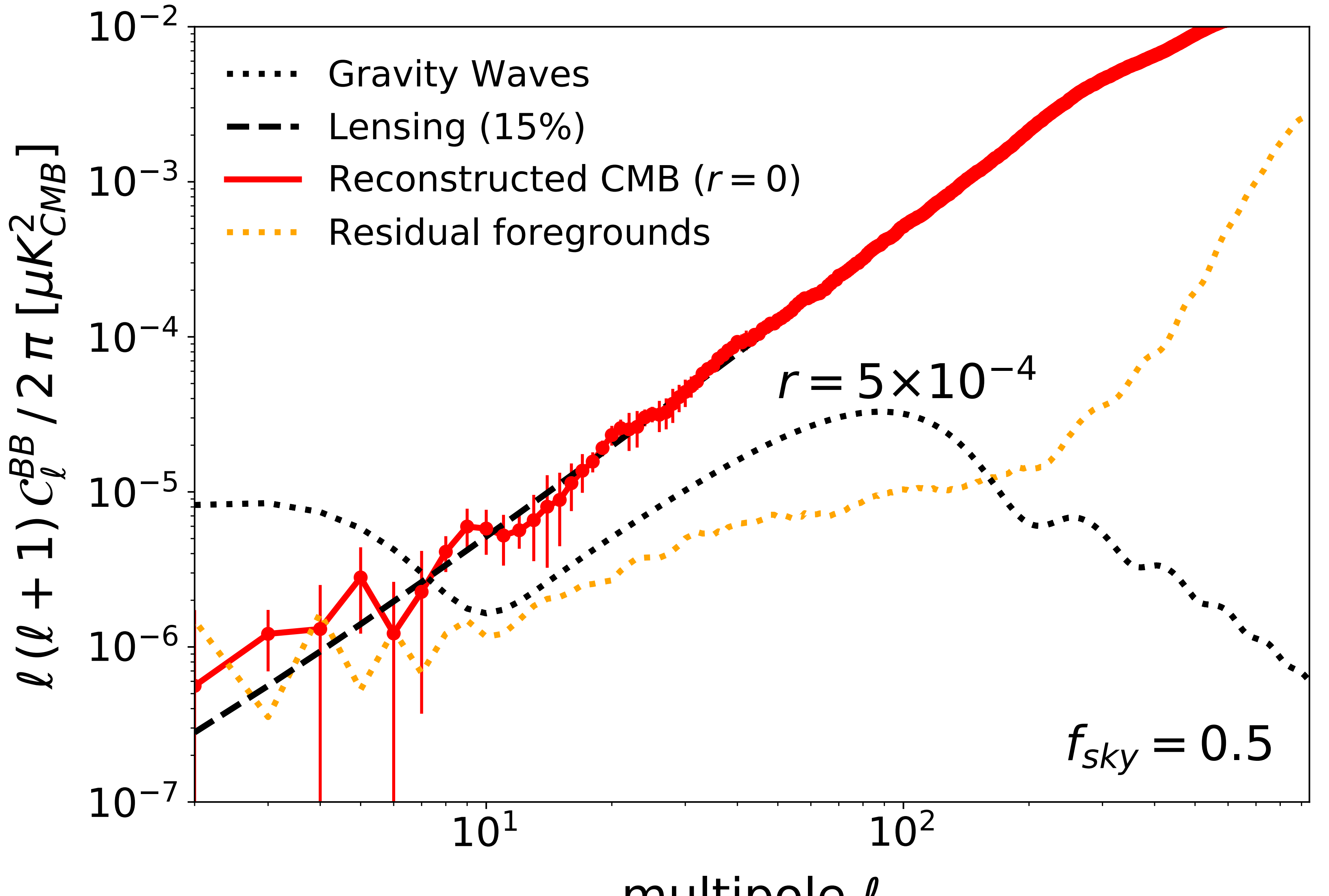

Figure: Remazeilles

- Bottom left: reconstructing CMB and foregrounds with 21 bands has no r bias (r=0.001)
- Bottom right: removing low/high frequencies introduces bias

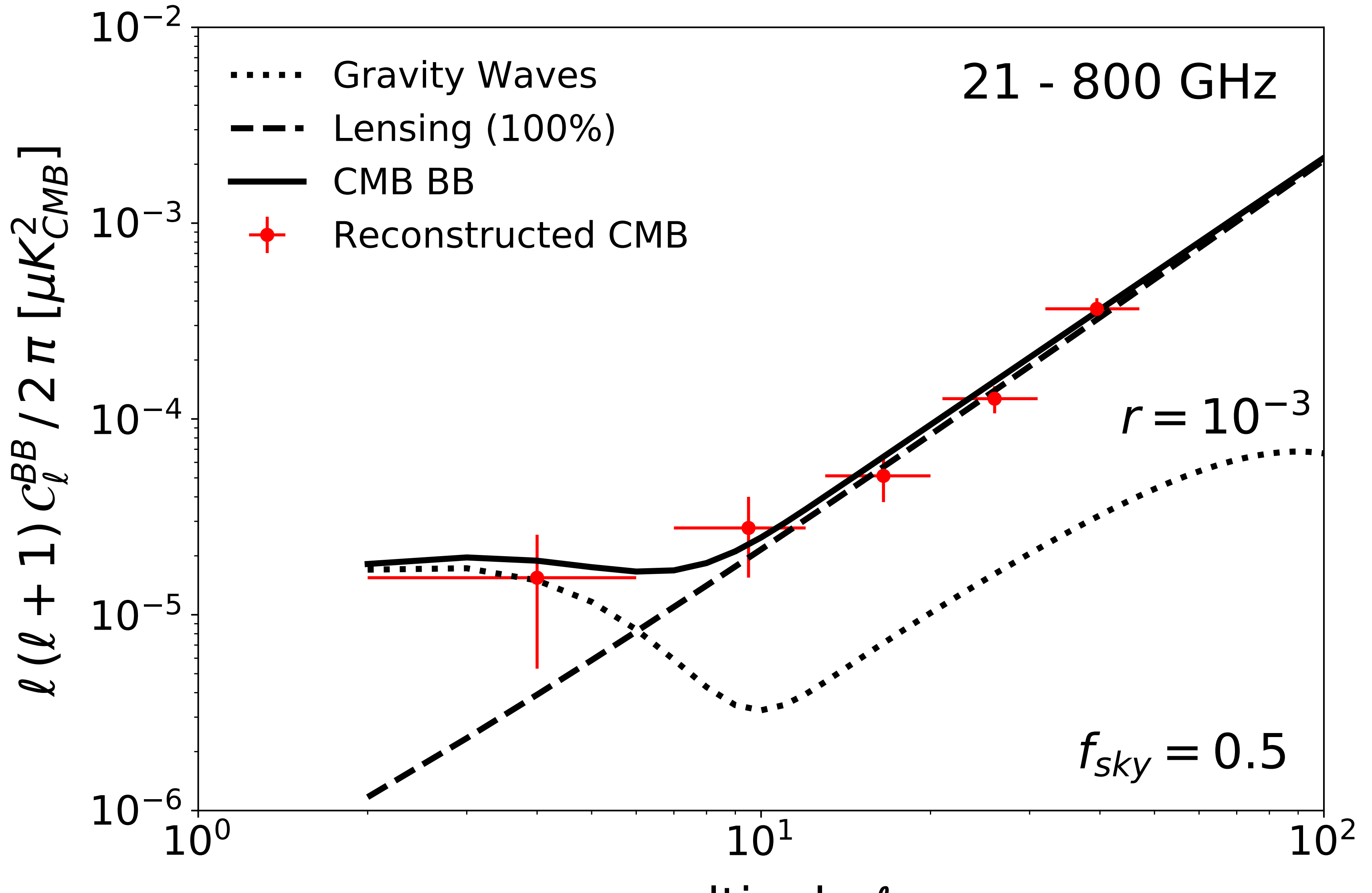

Figure: Remazeilles

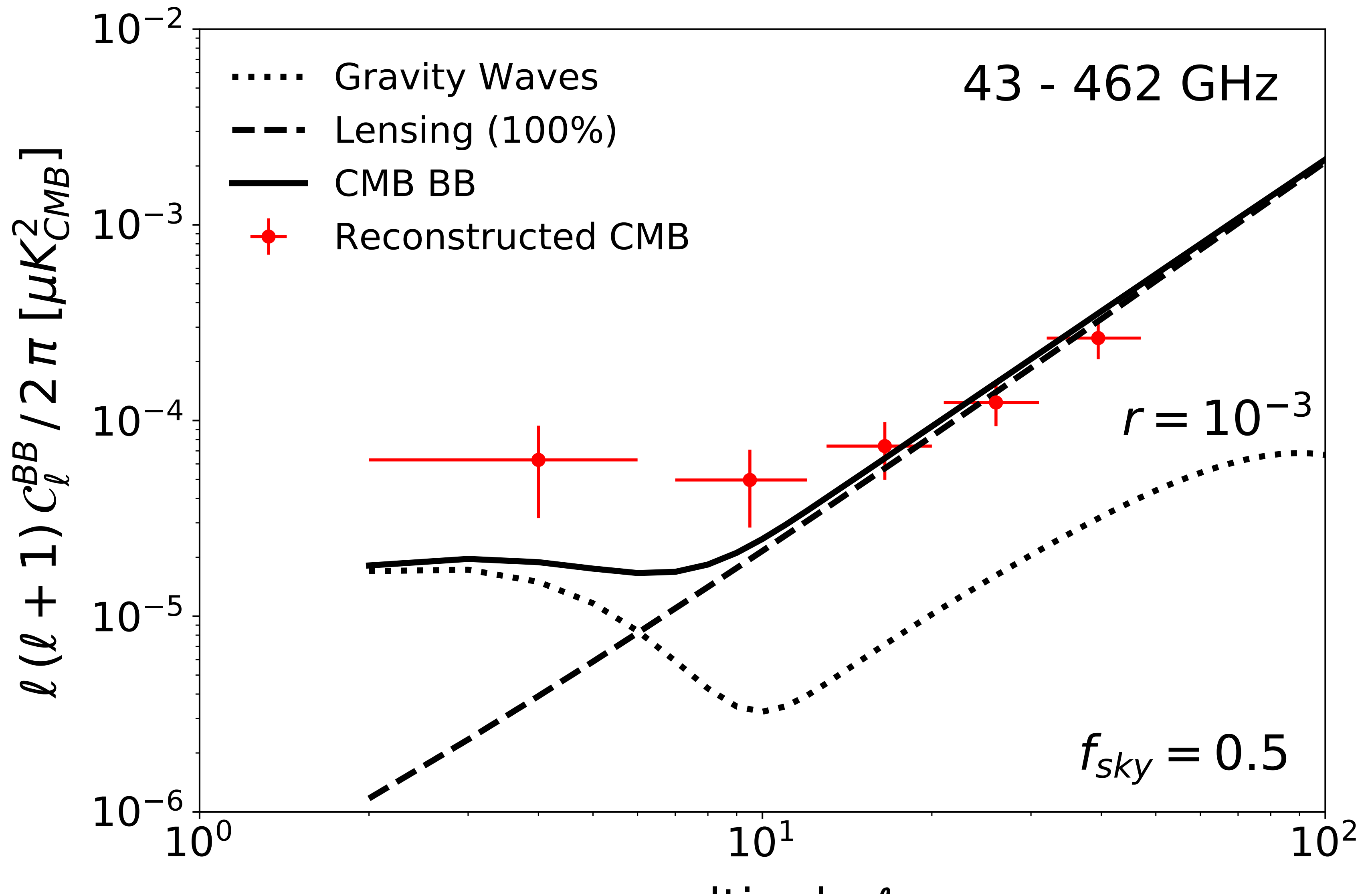

Figure: Remazeilles

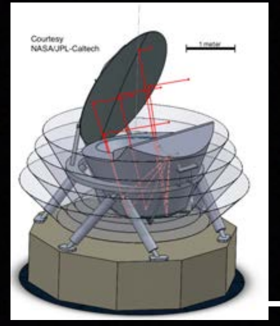

Simple Foreground Model

- 2 component dust model (a-la Finkbeiner et al)
- Synchrotron with power law frequency dependence
- ℓ dependence consistent with Planck and WMAP
- Includes correlation between dust and synchrotron, consistent with current data
- Model does not include:
  - spatial variation of the spectral index
  - spatial variation of dust temperature
- Foreground separation based on ILC
- 40% of sky (70% of sky reduces $\sigma(r)$)

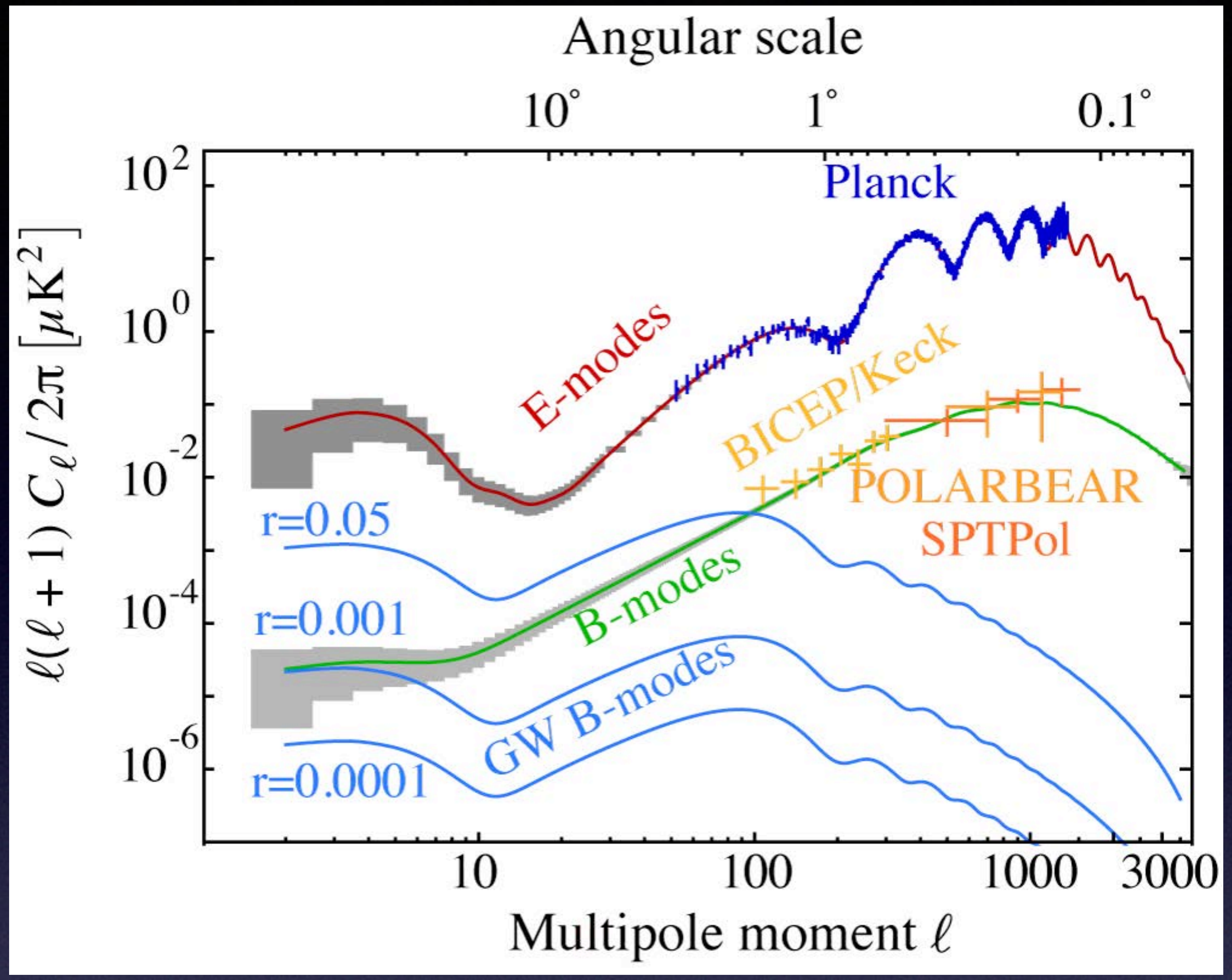

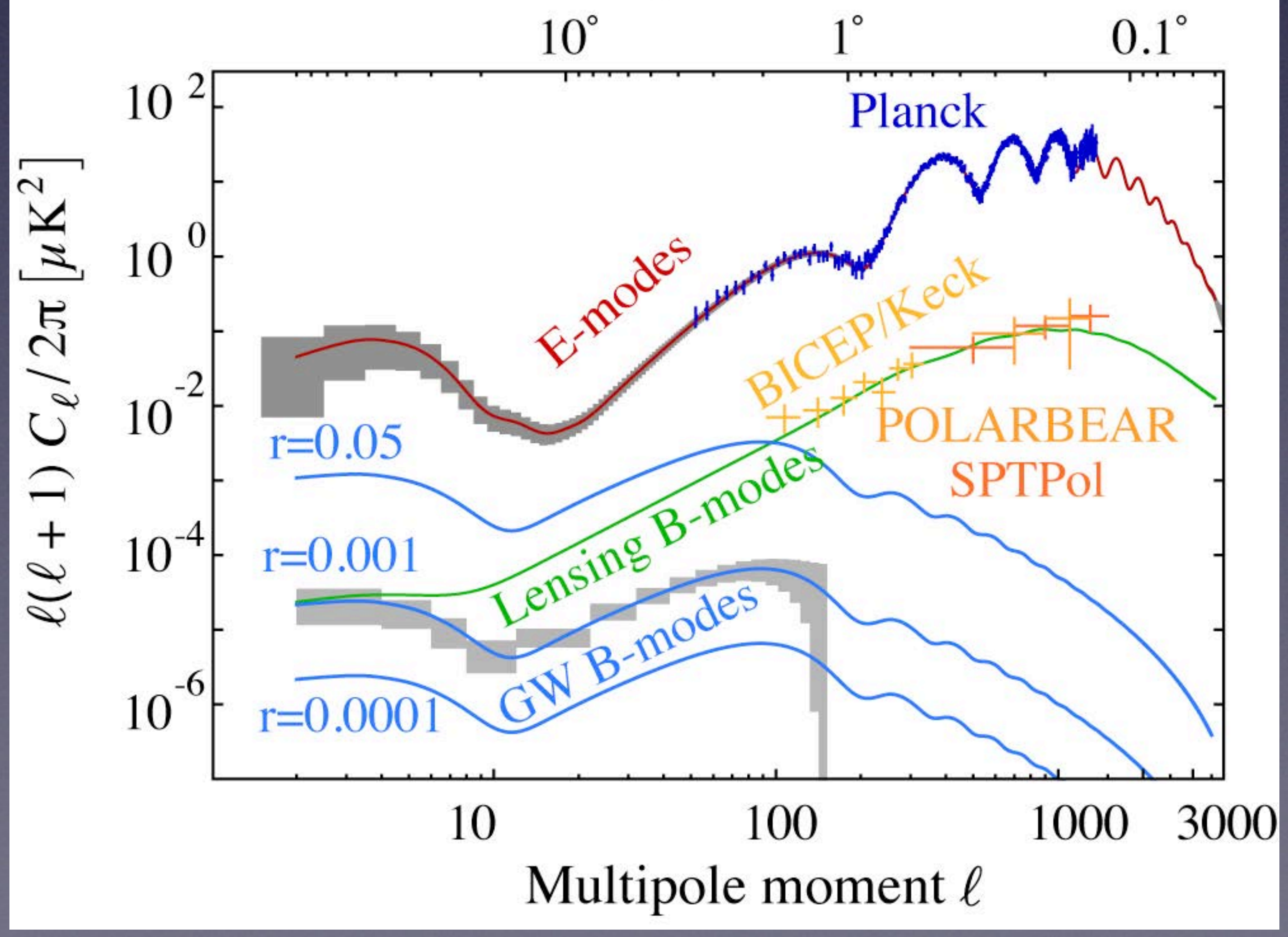

Figure: R. Flauger

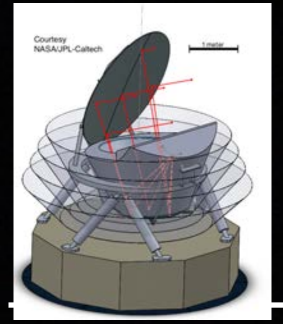

PICO Implementation

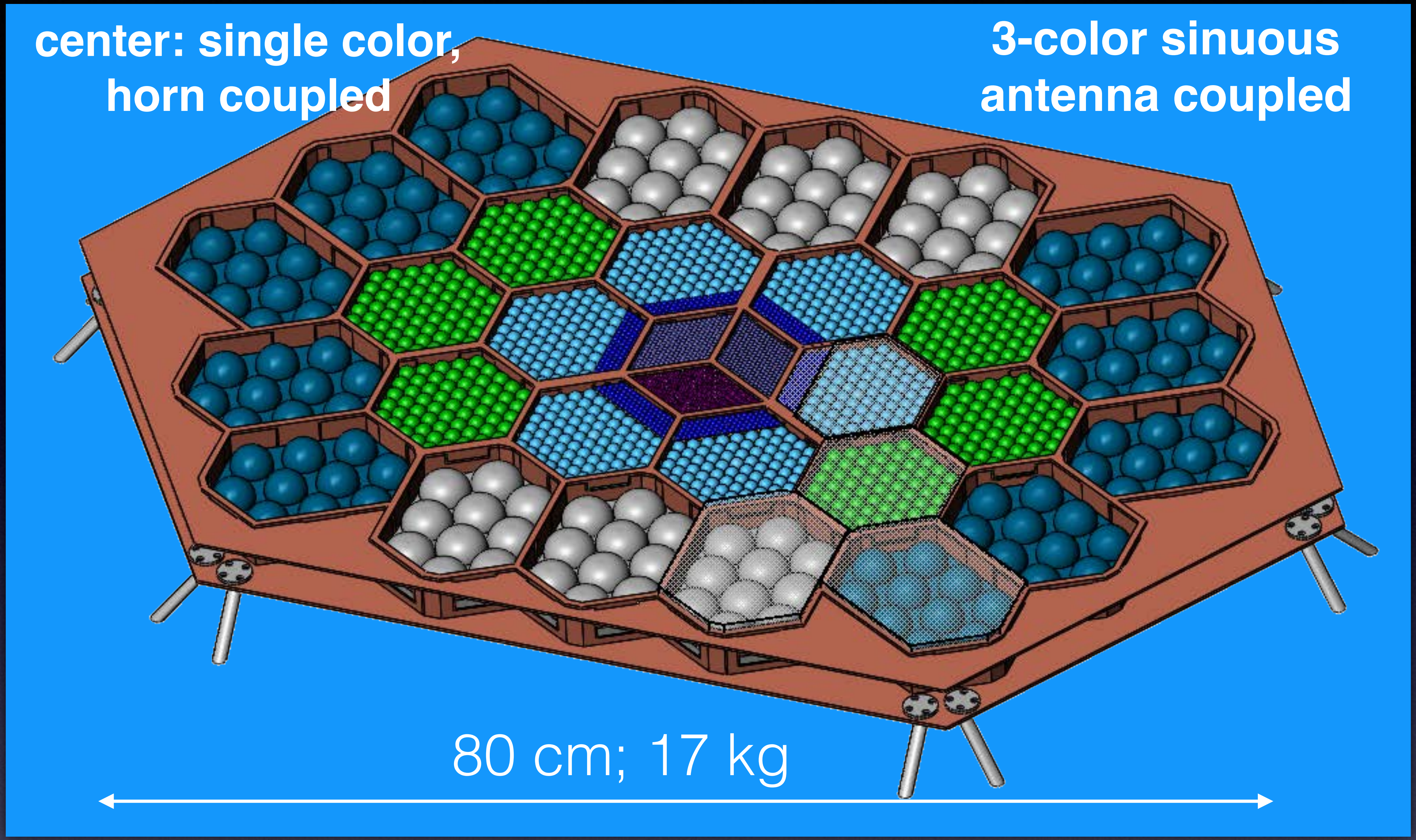

Tile type	N_{tile}	Pixels/ tile	Pixel type	Bandcenters [GHz]	Sampling rate [Hz]
1	6	10	A	21, 30, 43	45
2	10	10	B	25, 36, 52	55
3	6	61	C	62, 90, 129	136
4	6	85	D	75, 108, 155	163
		80	E	186, 268, 385	403
5	2	450	F	223, 321, 462	480
6	1	220	G	555	917
		200	H	666	
		180	I	799	

- A two-band/pixel focal plane design also available
- 19 bands, same noise (bands are broader, but less spill-over on stop)
- A monochroic focal plane design also available
- 21 band, higher noise but within requirements (only 20% margin)

Time Domain Multiplexing
128 x 102; 75 W

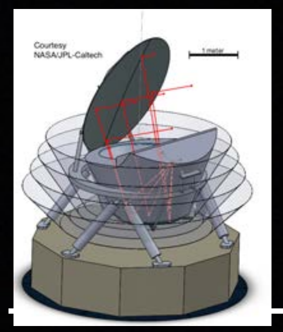

PICO Implementation - 2 Bands

- 19 bands, same noise (bands are broader, but less spill-over on stop-> higher efficiency)
- Corrugated feeds with dipole antenna (NIST+)

Pixel	Bands	# of Pixels	# of bolos/ band	# of bolos
A	21, 31	30	60	120
B	26, 38	50	100	200
C	47, 70	170	340	680
D	59, 87	250	500	1000
E	108, 161	400	800	1600
F	135, 200	410	820	1640
G	248, 368	320	640	1280
H	308, 458	280	560	1120
I	555	220	440	440
J	666	200	400	400
K	799	180	360	360
				8840

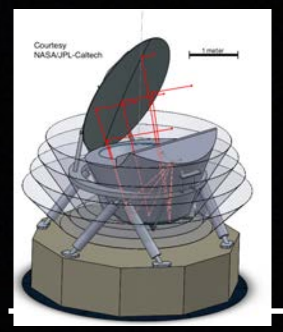

PICO Implementation - Monochromatic Pixels

- 21 bands, 20% higher noise (0.74 uK*arcmin), but within requirements (with less margin)
- Relies on higher packing density
- Phased dipole slot antennas (JPL)

band	nu	# of Pixels	# of bolos
1	20.8	30	60
2	25	35	70
3	30	40	80
4	36	45	90
5	43.2	50	100
6	51.8	55	110
7	62.2	160	320
8	74.6	175	350
9	89.6	200	400
10	107.5	230	460
11	129	270	540
12	154.8	300	600
13	185.8	270	540
14	222.9	250	500
15	267.5	240	480
16	321	230	460
17	385.2	210	420
18	462.2	180	360
19	554.7	110	220
20	665.6	100	200
21	798.7	90	180
			6540

PICO Additional Science

Figure: R. Flauger

- Dark matter / Axions:
  - 25 times stronger constraints than Planck, for ~MeV mass, not constrainable by direct detection experiments
  - x10 stronger constraints than Planck on axion mass between 10^{-26} and 10^{-30} eV
- Rule out primordial magnetic fields as source of largest galactic magnetic field Figure: R. Flauger
- Improve by x300 constraints on rotations due cosmic birefringence
- Source Catalog for Evolution of Structure:
  - 4500 strongly lensed galaxies (z up to 5)
  - 50,000 proto-clusters (z up to 4.5)
  - 30,000 dusty galaxies (z<0.1)